UNIVERSITY OF SASKATCHEWAN

NSERC
CRSNG

D(γ, n)H: Photodisintegration of the Deuteron at 18 MeV using Linearly Polarized Photons

Glen Pridham

June 24th, 2014

Outline

1. Introduction
2. Background
3. Experimental Setup
4. Analysis Methodology
5. Results and Discussion
6. Conclusion

Outline

1. Introduction ←
2. Background
3. Experimental Setup
4. Analysis Methodology
5. Results and Discussion
6. Conclusion

Introduction

In October 2010, we performed a deuteron photodisintegration experiment at the High-Intensity Gamma Source ($\mathrm{HI}\gamma S$) Free-Electron Laser (FEL) at Duke University in Durham, North Carolina.

The unpolarized deuterons were disintegrated by 18 MeV horizontally polarized photons; the recoil proton was ignored and the ejectile neutron was measured by Blowfish: a detector array of 88 BC-505 organic scintillators (i.e. $\mathrm{D}(\gamma, n)\mathrm{H}$).

$$\gamma + \mathrm{D} \longrightarrow n + \mathrm{H}$$

Introduction: Why?

Historical agreement between different experiments has been dubious at best; the scapegoat: Bremsstrahlung beams.

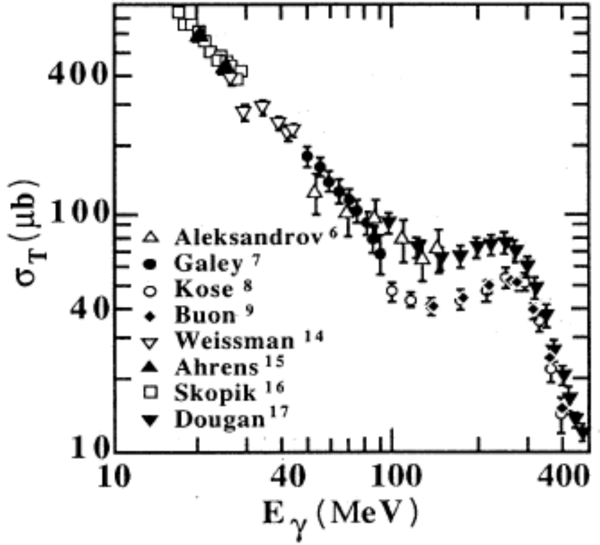

Before 1985

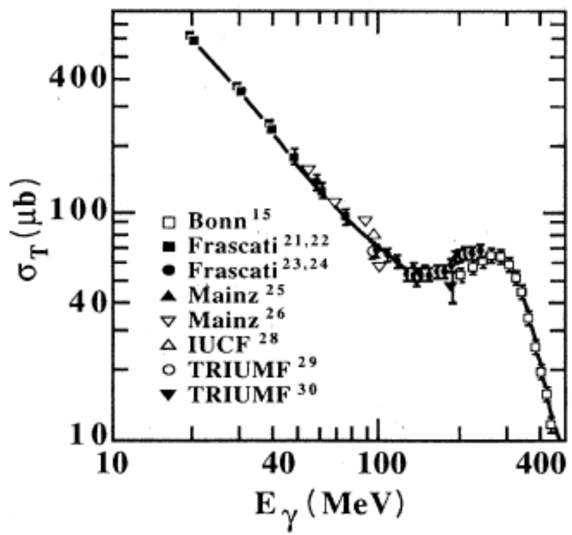

“Monochromatic” sources (after 1985)

Image credit: Rossi et al. (1989)

Introduction: Why?

Historical agreement between different experiments has been dubious at best; the scapegoat: Bremsstrahlung beams.

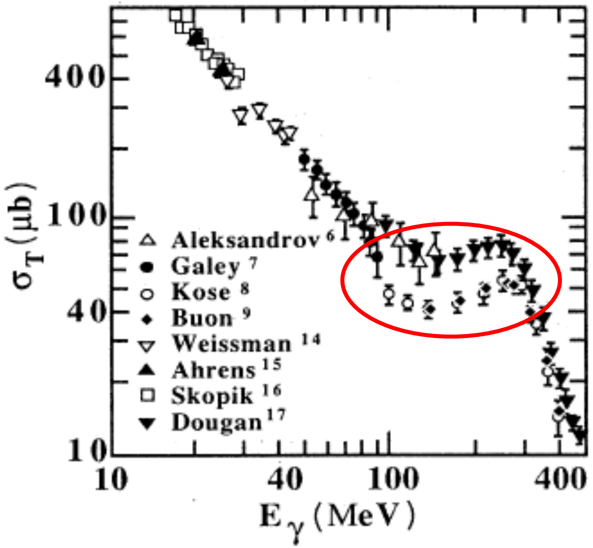

Before 1985

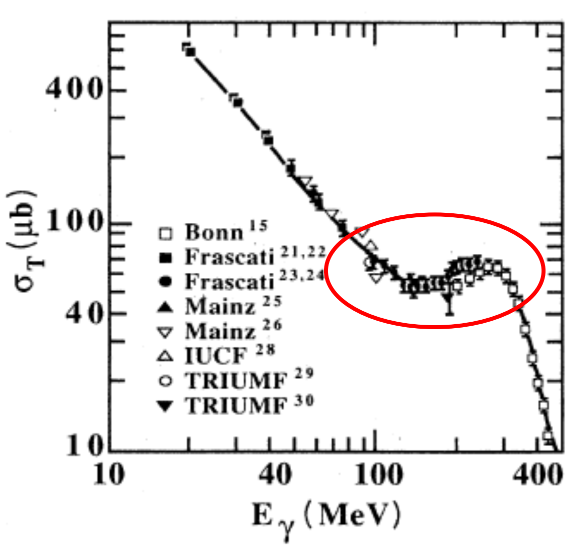

“Monochromatic” sources (after 1985)

Image credit: Rossi et al. (1989)

Introduction: Why?

Even “monochromatic” data don’t agree well with theory near energy threshold (2.2 MeV) nor at extreme angles (θ ~ 0°, 90° or 180°).

- - - - Then Contemporary Theory (Arenhövel, 2000)

— Older Theory (Partovi, 1964)

◇ Sawatzky (2005)

● Birenbaum et al. (1988)

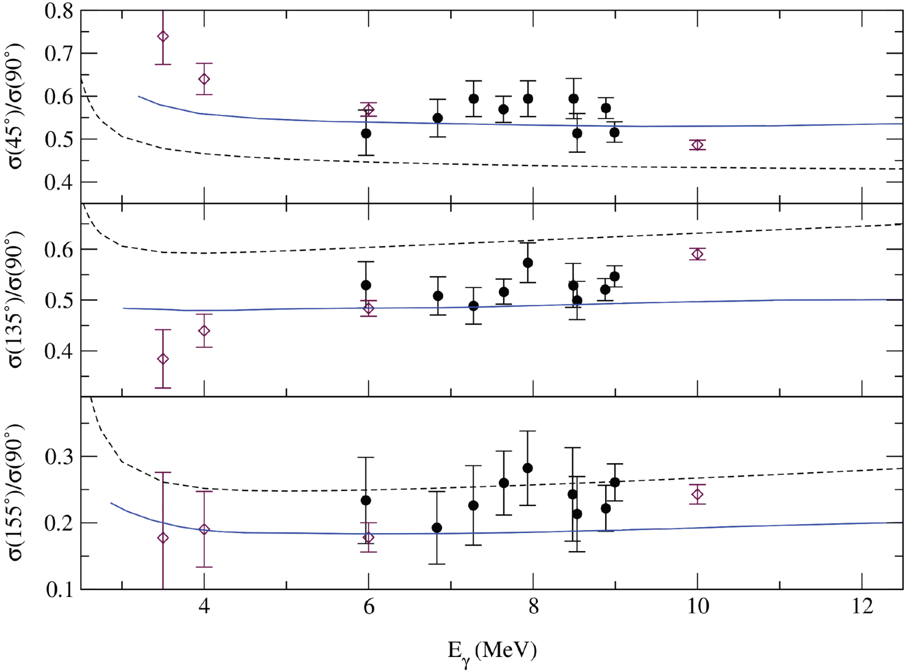

Image credit: Sawatzky (2005)

Introduction: Why?

Even “monochromatic” data don’t agree well with theory near energy threshold (2.2 MeV) nor at extreme angles (θ ~ 0°, 90° or 180°).

- - - - Then Contemporary Theory (Arenhövel, 2000)

—— Older Theory (Partovi, 1964)

◇ Sawatzky (2005)

● Birenbaum et al. (1988)

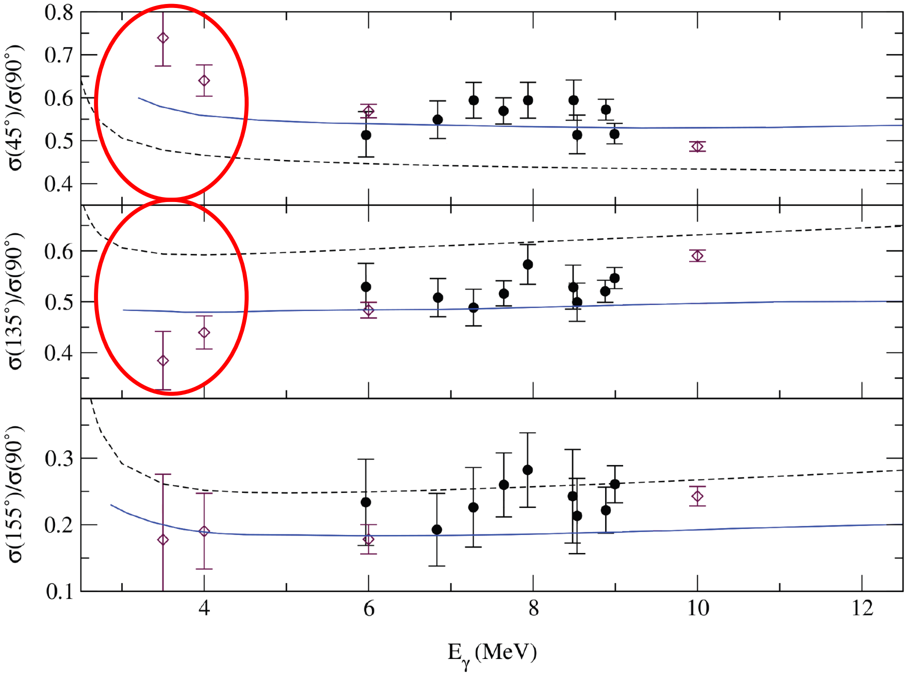

Image credit: Sawatzky (2005)

Outline

1. Introduction
2. Background ⬅
3. Experimental Setup
4. Analysis Methodology
5. Results and Discussion
6. Conclusion

Background: Elster Nucleon-Nucleon Potential

Based on the 1987 Bonn r-potential: a position-space single meson exchange potential including *π, σ, η, ω, δ,* and *ρ* mesons.

Additional corrections were made to extend the Bonn potential above pion threshold, including: meson retardation effects, nucleon self-energy diagrams, and delta baryon intermediate states.

Background: The Calculation

Schwamb and Arenhövel performed the calculation for $\mathrm{D}(\gamma, n)\mathrm{H}$ (the reaction we tested).

They used a non-relativistic deuteron based on the Elster potential, then calculated the reaction, including: retarded meson exchange, the delta baryon degree-of-freedom, off-shell mesons, and relativistic corrections.

Background: The Calculation

Schwamb and Arenhövel performed the calculation for $\mathrm{D}(\gamma, n)\mathrm{H}$ (the reaction we tested).

They used a non-relativistic deuteron based on the Elster potential, then calculated the reaction, including: retarded meson exchange, the delta baryon degree-of-freedom, off-shell mesons, and relativistic corrections.

Mesons transfer information at c

Background: The Calculation

Schwamb and Arenhövel performed the calculation for $\mathrm{D}(\gamma, n)\mathrm{H}$ (the reaction we tested).

They used a non-relativistic deuteron based on the Elster potential, then calculated the reaction, including: retarded meson exchange, the delta baryon degree-of-freedom, off-shell mesons, and relativistic corrections.

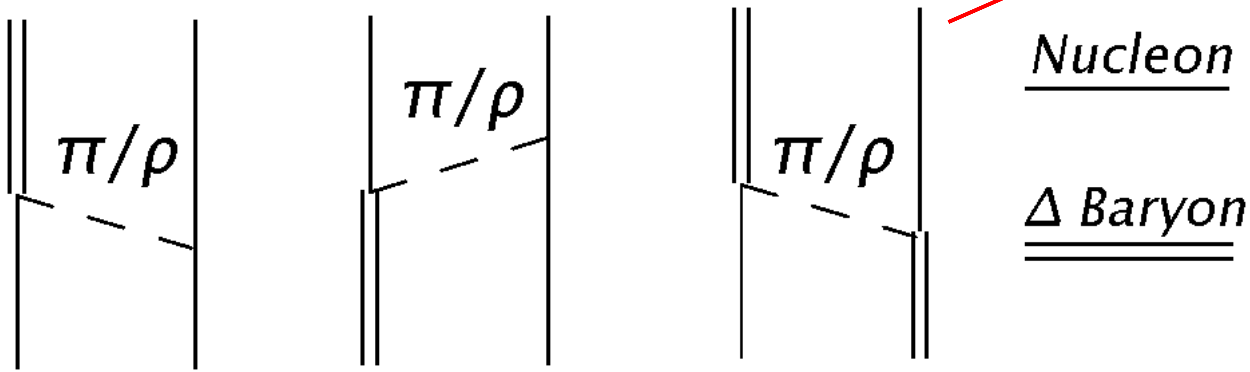

Background: The Calculation

Schwamb and Arenhövel performed the calculation for $\mathrm{D}(\gamma, n)\mathrm{H}$ (the reaction we tested).

They used a non-relativistic deuteron based on the Elster potential, then calculated the reaction, including: retarded meson exchange, the delta baryon degree-of-freedom, off-shell mesons, and relativistic corrections.

e.g.

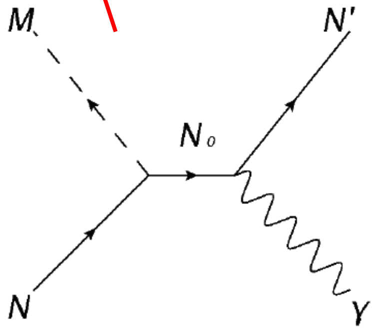

Background: The Calculation

Schwamb and Arenhövel performed the calculation for $\mathrm{D}(\gamma, n)\mathrm{H}$ (the reaction we tested).

They used a non-relativistic deuteron based on the Elster potential, then calculated the reaction, including: retarded meson exchange, the delta baryon degree-of-freedom, off-shell mesons, and relativistic corrections.

Spin effects and corrections to non-relativistic deuteron wavefunction

Background: The Calculation

Schwamb and Arenhövel performed the calculation for $\mathrm{D}(\gamma, n)\mathrm{H}$ (the reaction we tested).

They used a non-relativistic deuteron based on the Elster potential, then calculated the reaction, including: retarded meson exchange, the delta baryon degree-of-freedom, off-shell mesons, and relativistic corrections.

They calculated a slew of observables, we can compare our results to their: cross section (σ), φ-averaged differential cross section ($\mathrm{d}\sigma/\mathrm{d}\Omega(\theta)$), and analyzing power ($\Sigma(\theta)$).

Background: The Calculation

Schwamb and Arenhövel performed the calculation for $\mathrm{D}(\gamma, n)\mathrm{H}$ (the reaction we tested).

They used a non-relativistic deuteron based on the Elster potential, then calculated the reaction, including: retarded meson exchange, the delta baryon degree-of-freedom, off-shell mesons, and relativistic corrections.

They calculated a slew of observables, we can compare our results to their: cross section (σ), φ-averaged differential cross section ($d\sigma/d\Omega(\theta)$), and analyzing power ($\Sigma(\theta)$).

$$\Sigma(\theta) \equiv \frac{1}{\Sigma^l} \frac{\frac{d\sigma}{d\Omega}(\theta, \phi = 0^\circ) - \frac{d\sigma}{d\Omega}(\theta, \phi = 90^\circ)}{\frac{d\sigma}{d\Omega}(\theta, \phi = 0^\circ) + \frac{d\sigma}{d\Omega}(\theta, \phi = 90^\circ)}$$

Outline

1. Introduction
2. Background
3. Experimental Setup ←
4. Analysis Methodology
5. Results and Discussion
6. Conclusion

Experiment: Beam

The High-Intensity Gamma Source ($\mathrm{HI}\gamma S$) at Duke University

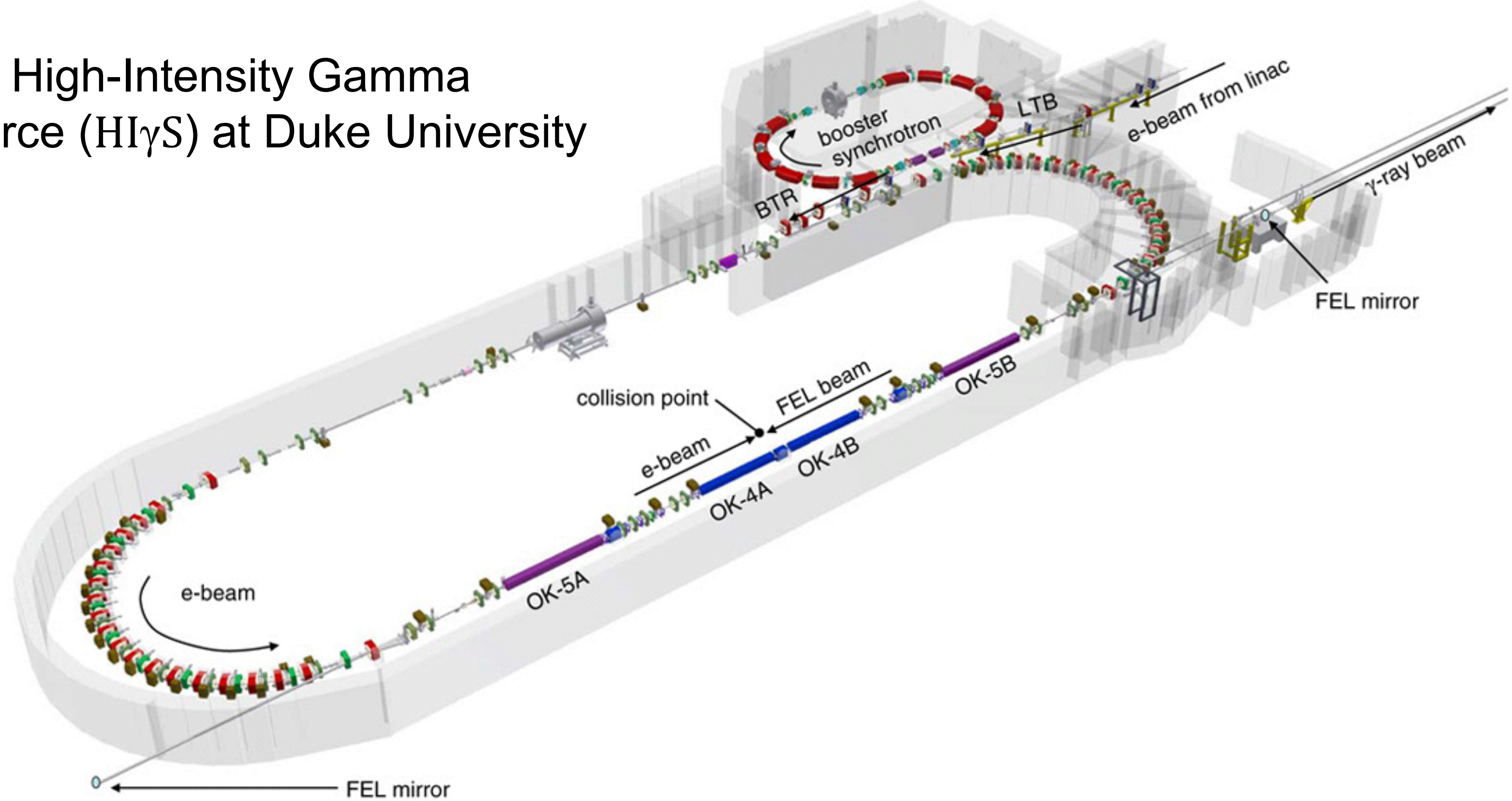

Image credit: Weller et al. (2009)

Experiment: Beam

The High-Intensity Gamma Source (HIγS) at Duke University

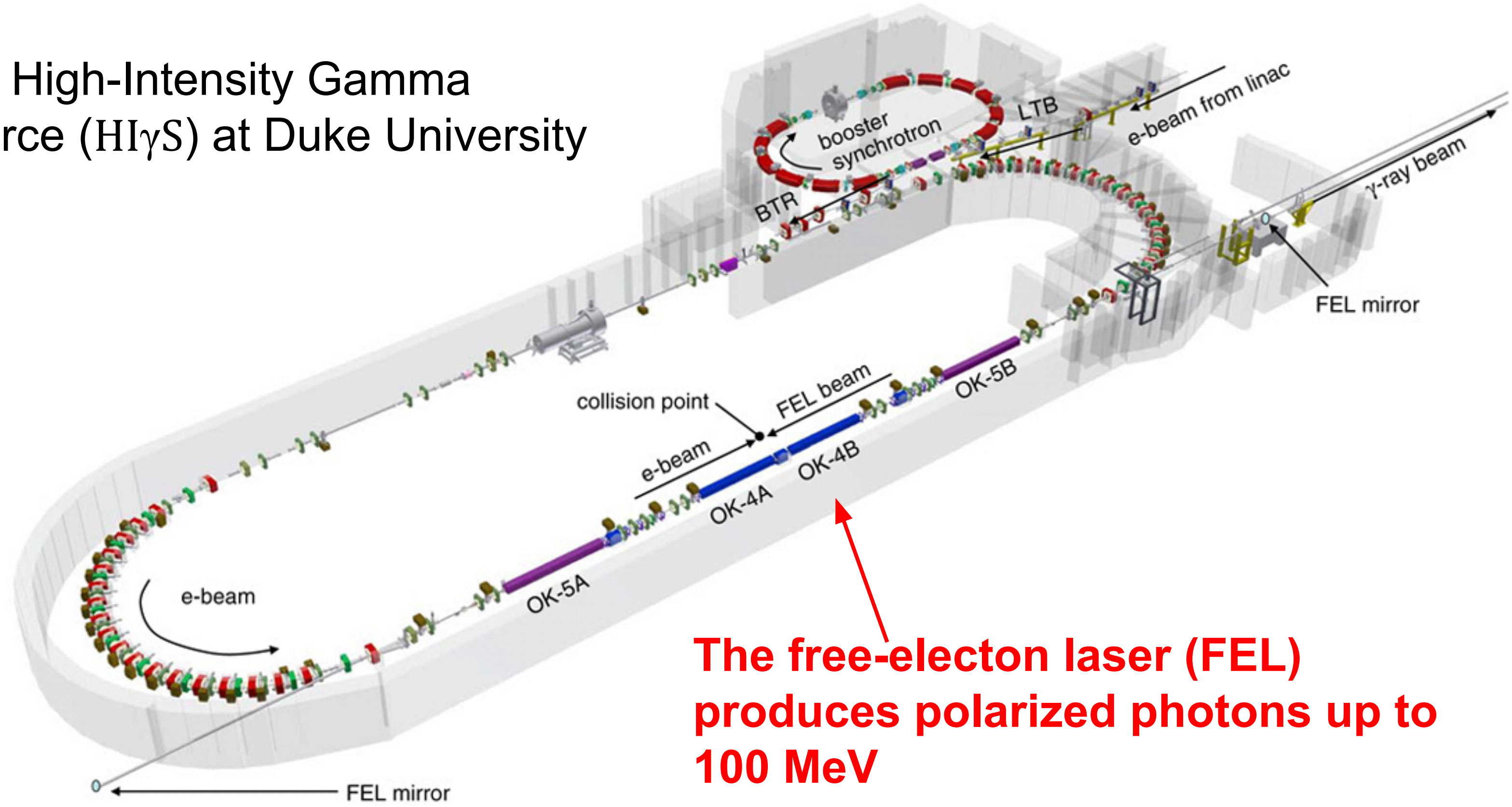

The free-electon laser (FEL) produces polarized photons up to 100 MeV

Image credit: Weller et al. (2009)

Experiment: Detectors

Blowfish:

88 BC-505 liquid organic scintillators covering ~π steradians over polar angles $\theta \in$ [22.5°, 157.5°] and azimuthal angles $\varphi \in$ [0°, 360°).

Purpose:

to measures photons and neutrons from the target.

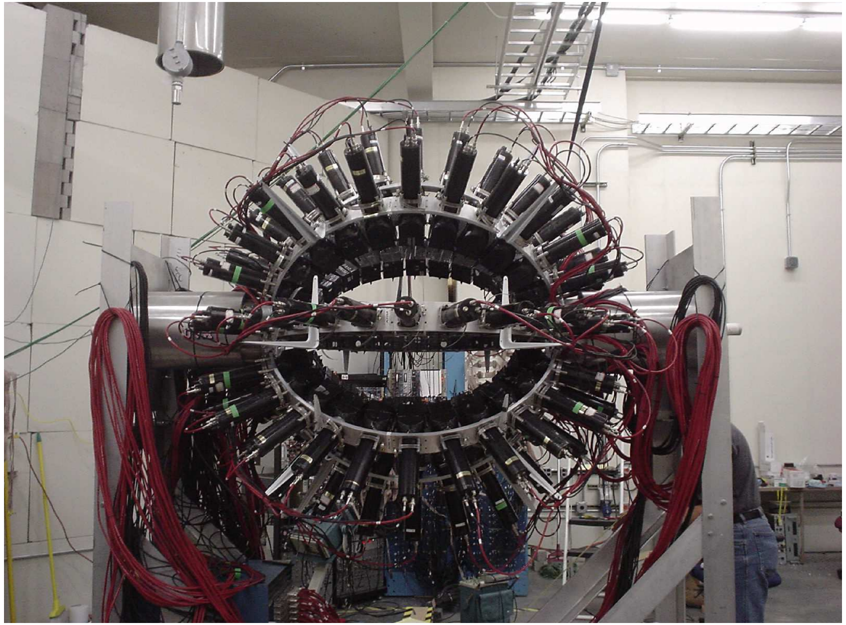

Image credit: Sawatzy (2005)

Brad Sawatzky proudly poses with Blowfish

Experiment: Detectors

The Five Paddle Flux Monitor:

five 2 mm wide BC-400 solid organic scintillator paddles and a 2 mm wide aluminum radiator.

Purpose:

to estimate the number of beam photons reaching the target.

Calibrated by a sodium iodide crystal placed in the beam-line periodically.

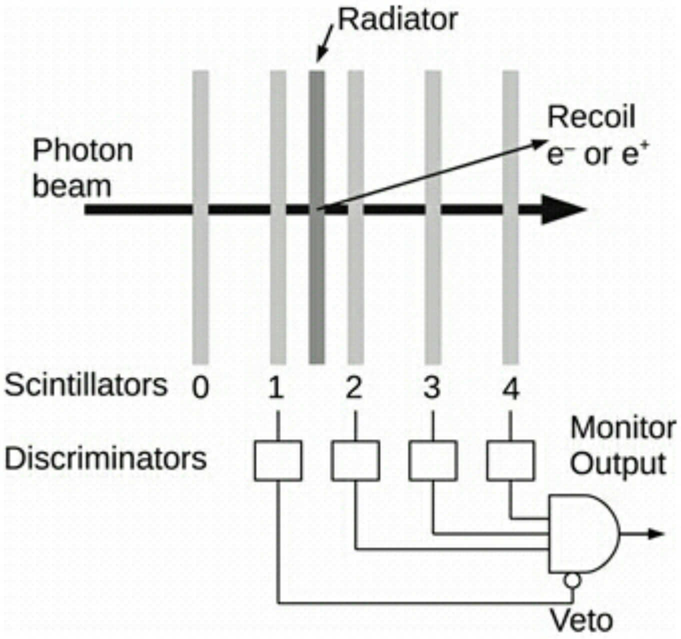

Image credit: Mavrichi (2010)

Experiment: Targets

Deuteron targets:

Lucite vials filled with D_2O in two lengths: 10.7 cm and 2 cm.

Background target:

a 10.7 cm H_2O target was also used in order to measure neutrons from sources other than the deuteron.

Image credit: Kucuker (2010)

Experiment: Layout

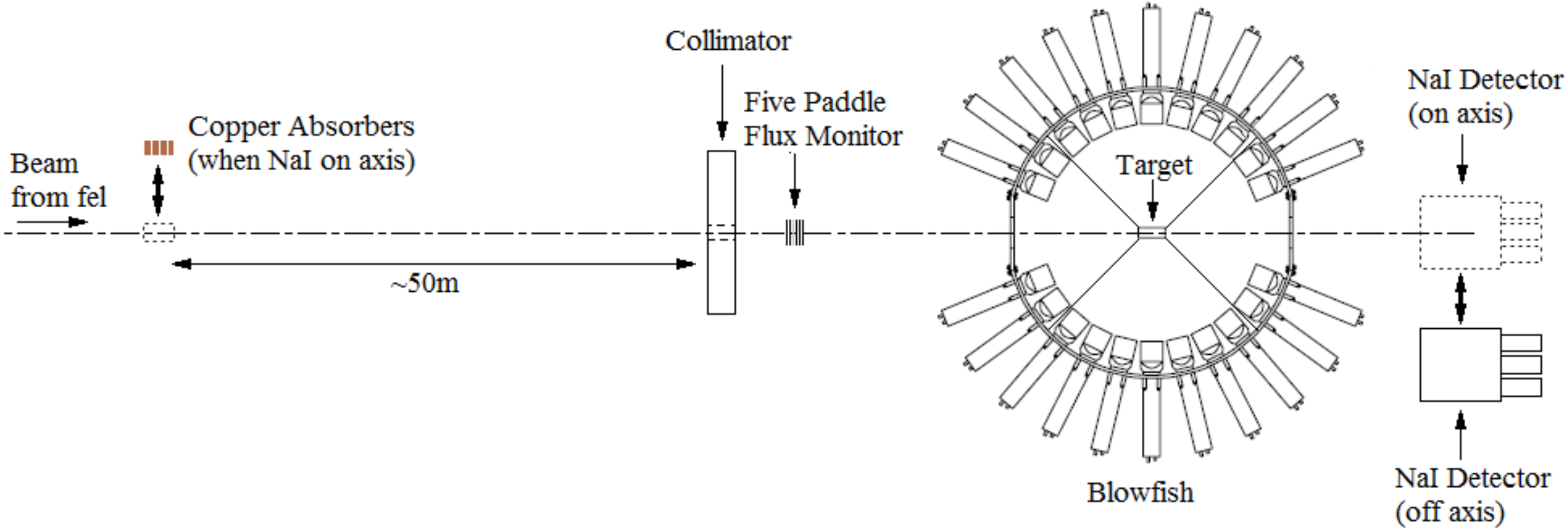

Outline

1. Introduction
2. Background
3. Experimental Setup
4. Analysis Methodology ←
5. Results and Discussion
6. Conclusion

Analysis: Processing the Data

Using the data analysis software system ROOT, we processed our data from Blowfish using the following cuts (in order):

1. Multiplicity to remove concurrent events.
2. Pulse-shape discrimination to remove photon events.
3. Energy (detector response).
4. Time-of-flight based on kinematics.
5. Background radiation count.

Finally, we use a water target correction to account for any noise left after all other cuts were applied. This gives us a final neutron yield.

Analysis: Differential Cross Section

Cambi et al. (1982) showed that the theoretical calculation can be parameterized in terms of associated Legendre polynomials:

$$\frac{d\sigma}{d\Omega}(\theta, \phi) = \sum_{k=0}^{n} A_k P_k^0(\cos\theta) + \sum_{k=2}^{n} B_k \Sigma_l P_k^2(\cos\theta)\cos 2\phi$$

Analysis: Comparing to Theory

First, we made a few adjustments to the expansion and truncated it:

$$\frac{d\sigma}{d\Omega}(\theta, \phi) = \sum_{k=0}^{n} A_k P_k^0(\cos\theta) + \sum_{k=2}^{n} B_k \Sigma_l P_k^2(\cos\theta) \cos 2\phi$$

$$\frac{d\sigma}{d\Omega} = \frac{\sigma}{4\pi}\left[1 + \sum_{k=1}^{4} a_k P_k^0(\cos\theta) + \sum_{k=2}^{4} e_k P_k^2(\cos\theta)\cos 2\phi\right.$$

$$\left.\ldots + \sum_{k=1}^{2} c_k P_k^1(\cos\theta)\cos\phi + \sum_{k=1}^{2} d_k P_k^1(\cos\theta)\sin\phi\right]$$

Target alignment terms

Analysis: Differential Cross Section

Next, we mapped the Legendre polynomials into probability density functions and simulated them (Monte Carlo), giving us an expansion in terms of neutron yields, *N*:

$$
\begin{aligned}
N_d =& A[(1-\sum_{k=1}^{4} a_k - 3e_2 - 6e_3 - 10e_4 - c_1 - \frac{3}{2}c_2 - d_1 - \frac{3}{2}d_2)N_{d,00}^{sim} \\
&... + \sum_{k=1}^{4} a_k N_{d,0k}^{sim} + 3e_2 N_{d,22}^{sim} + 6e_3 N_{d,23}^{sim} + 10e_4 N_{d,24}^{sim} \\
&... + c_1 N_{d,11}^{sim} + \frac{3}{2}c_2 N_{d,12}^{sim} + d_1 N_{d,11'}^{sim} + \frac{3}{2}d_2 N_{d,12'}^{sim}]
\end{aligned}
$$

Analysis: Differential Cross Section

Next, we mapped the Legendre polynomials into probability density functions and simulated them (Monte Carlo), giving us an expansion in terms of neutron yields, *N*:

$$
\begin{aligned}
N_d = & A[(1 - \sum_{k=1}^{4} a_k - 3e_2 - 6e_3 - 10e_4 - c_1 - \frac{3}{2}c_2 - d_1 - \frac{3}{2}d_2) N^{sim}_{d,00} \\
& \ldots + \sum_{k=1}^{4} a_k N^{sim}_{d,0k} + 3e_2 N^{sim}_{d,22} + 6e_3 N^{sim}_{d,23} + 10e_4 N^{sim}_{d,24} \\
& \ldots + c_1 N^{sim}_{d,11} + \frac{3}{2}c_2 N^{sim}_{d,12} + d_1 N^{sim}_{d,11'} + \frac{3}{2}d_2 N^{sim}_{d,12'}]
\end{aligned}
$$

Simulated yields

Analysis: Differential Cross Section

Finally, we fit our experimental neutron yield for each detector, *d*, to the function:

$$\begin{aligned} N_d =& A[(1 - \sum_{k=1}^{4} a_k - 3e_2 - 6e_3 - 10e_4 - c_1 - \frac{3}{2}c_2 - d_1 - \frac{3}{2}d_2) N_{d,00}^{sim} \\ & \ldots + \sum_{k=1}^{4} a_k N_{d,0k}^{sim} + 3e_2 N_{d,22}^{sim} + 6e_3 N_{d,23}^{sim} + 10e_4 N_{d,24}^{sim} \\ & \ldots + c_1 N_{d,11}^{sim} + \frac{3}{2}c_2 N_{d,12}^{sim} + d_1 N_{d,11'}^{sim} + \frac{3}{2}d_2 N_{d,12'}^{sim}] \end{aligned}$$

Analysis: Differential Cross Section

Finally, we fit our experimental neutron yield for each detector, *d*, to the function:

$$N_d = A[(1 - \sum_{k=1}^{4} a_k - 3e_2 - 6e_3 - 10e_4 - c_1 - \frac{3}{2}c_2 - d_1 - \frac{3}{2}d_2)N_{d,00}^{sim}$$

$$... + \sum_{k=1}^{4} a_k N_{d,0k}^{sim} + 3e_2 N_{d,22}^{sim} + 6e_3 N_{d,23}^{sim} + 10e_4 N_{d,24}^{sim}$$

$$... + c_1 N_{d,11}^{sim} + \frac{3}{2}c_2 N_{d,12}^{sim} + d_1 N_{d,11'}^{sim} + \frac{3}{2}d_2 N_{d,12'}^{sim}]$$

We have 88 detectors and 12 fit parameters.

Analysis: Differential Cross Section

We used GEANT4 (Monte Carlo) to account for confounding scattering/absorption processes.

We generated neutrons in the target with probabilistic density functions based on the associated Legendre Polynomials.

The simulation reproduces our experimental efficiency.

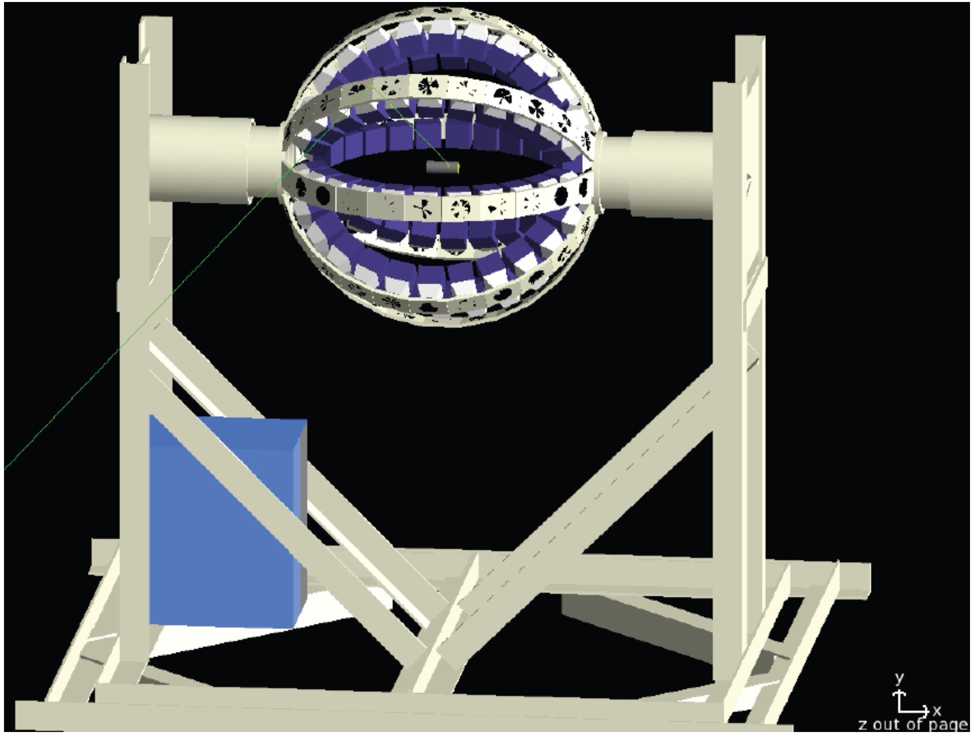

Analysis: Total Cross Section

Using the Five Paddle Flux Monitor we know the number of photons hitting the target.

Blowfish tells us the number of neutrons coming out of the target.

Our GEANT4 simulation tells us the *efficiency* of our Blowfish detectors.

Efficiency Test (Pywell et al, 2006)

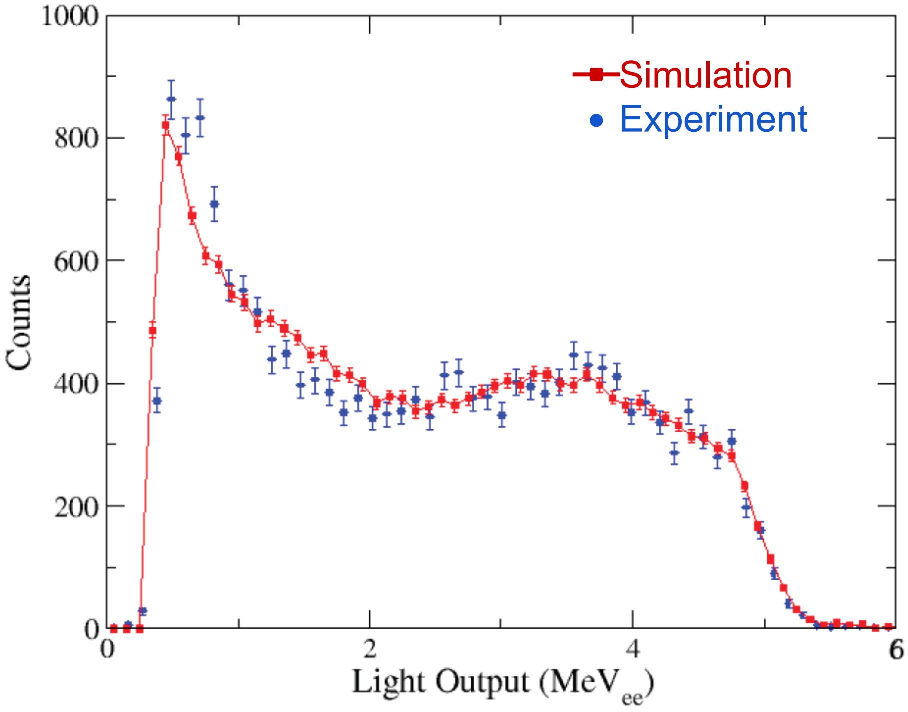

Analysis: Total Cross Section

Using the Five Paddle Flux Monitor we know the number of photons hitting the target.

Blowfish tells us the number of neutrons coming out of the target.

Our GEANT4 simulation tells us the *efficiency* of our Blowfish detectors.

σ

Efficiency Test (Pywell et al, 2006)

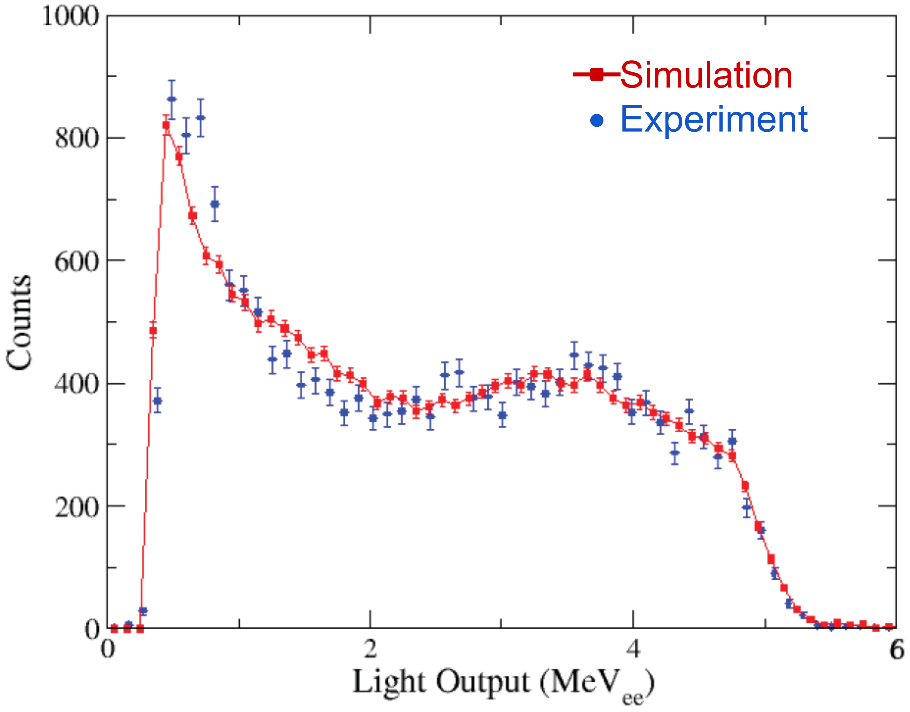

Outline

1. Introduction
2. Background
3. Experimental Setup
4. Analysis Methodology
5. Results and Discussion ⬅
6. Conclusion

Results: Total Cross Section

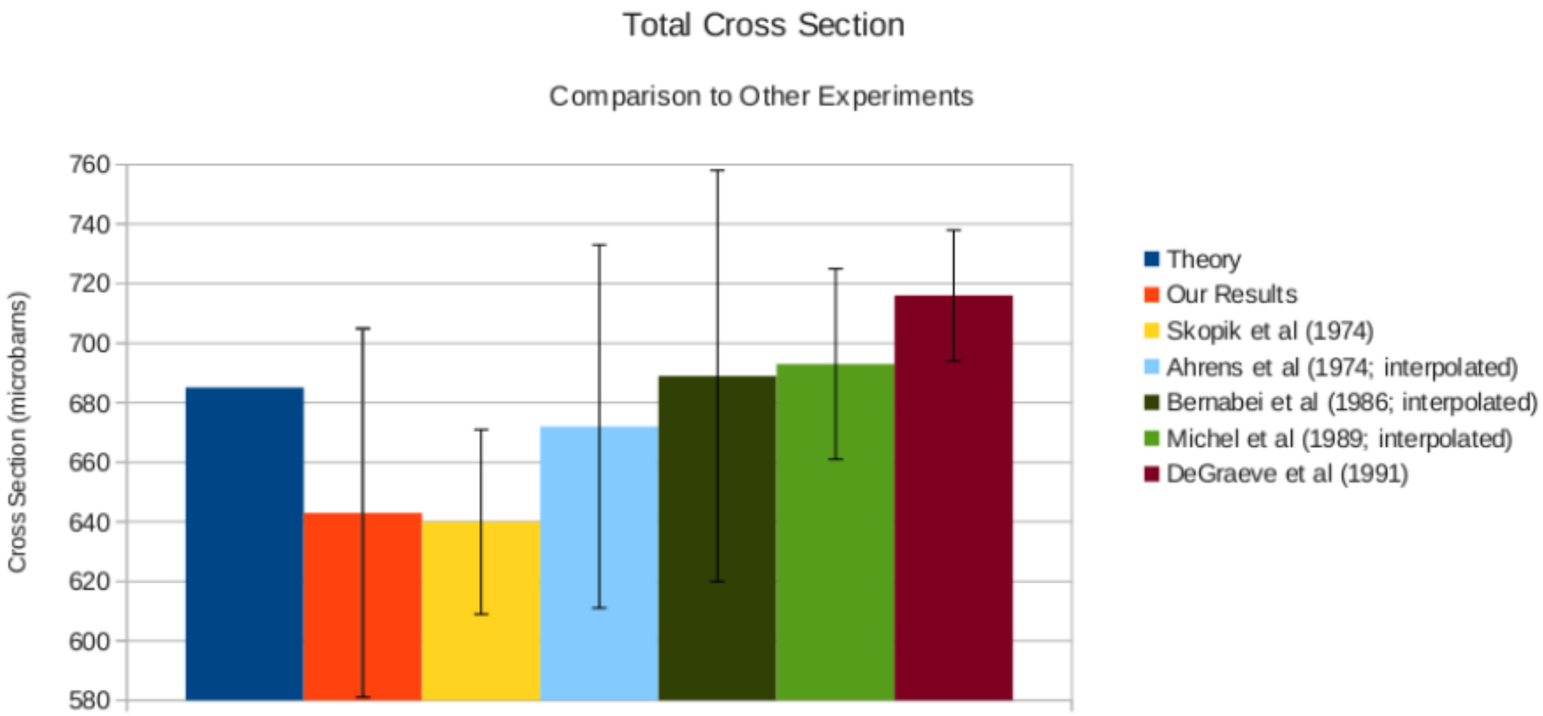

Results: Total Cross Section

Our results are lower than expected, but agree with everybody (within error)

Total Cross Section

Comparison to Other Experiments

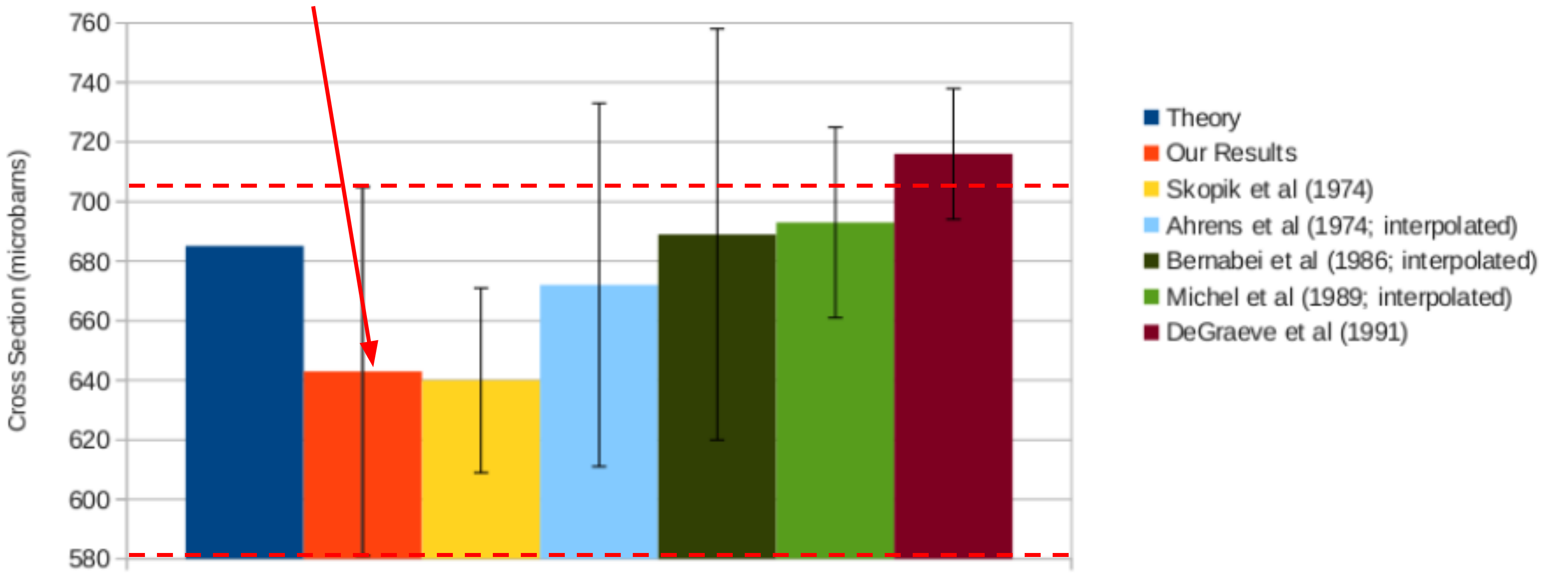

Results: Total Cross Section

Our results are lower than expected, but agree with everybody (within error)

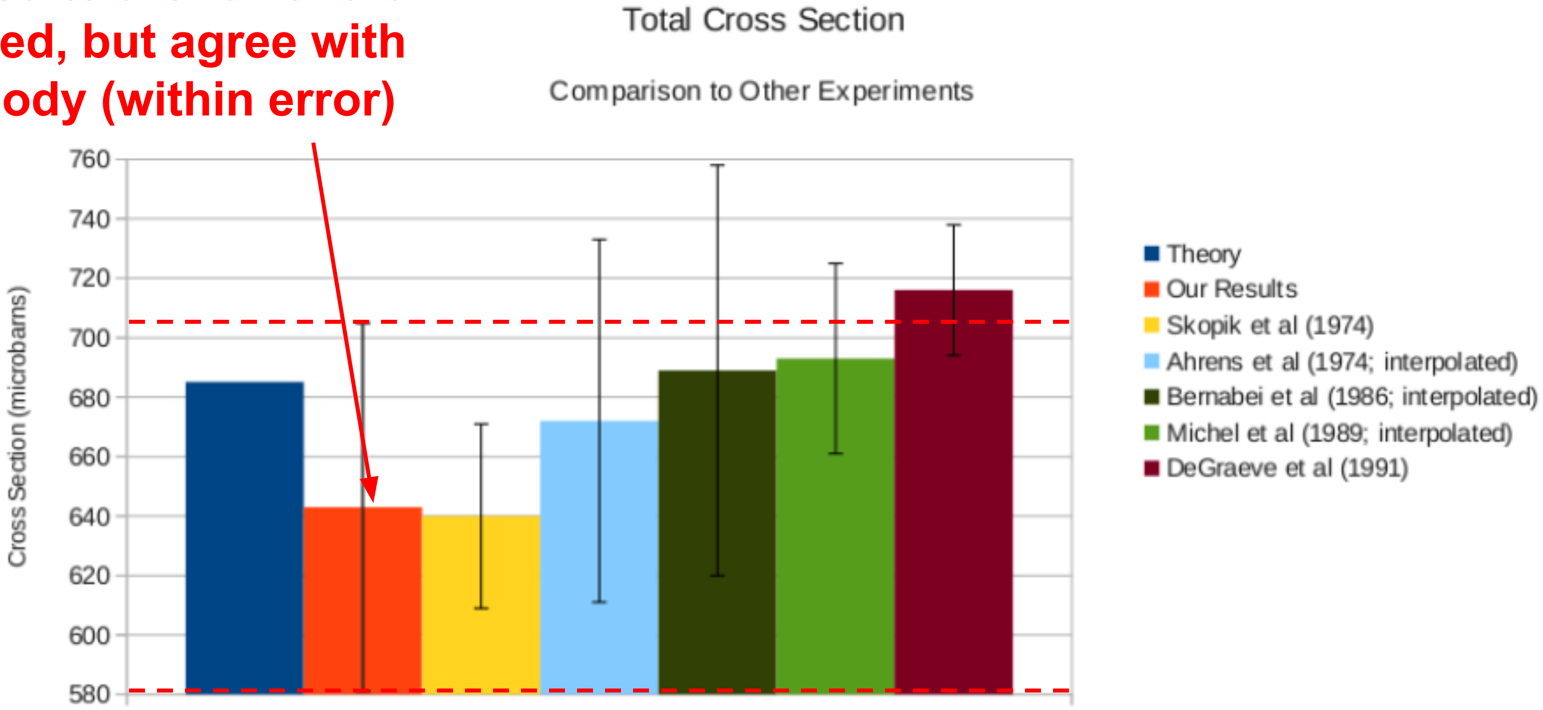

Note: suppressed zero

Results: Total Cross Section

Our results are lower than expected, but agree with everybody (within error)

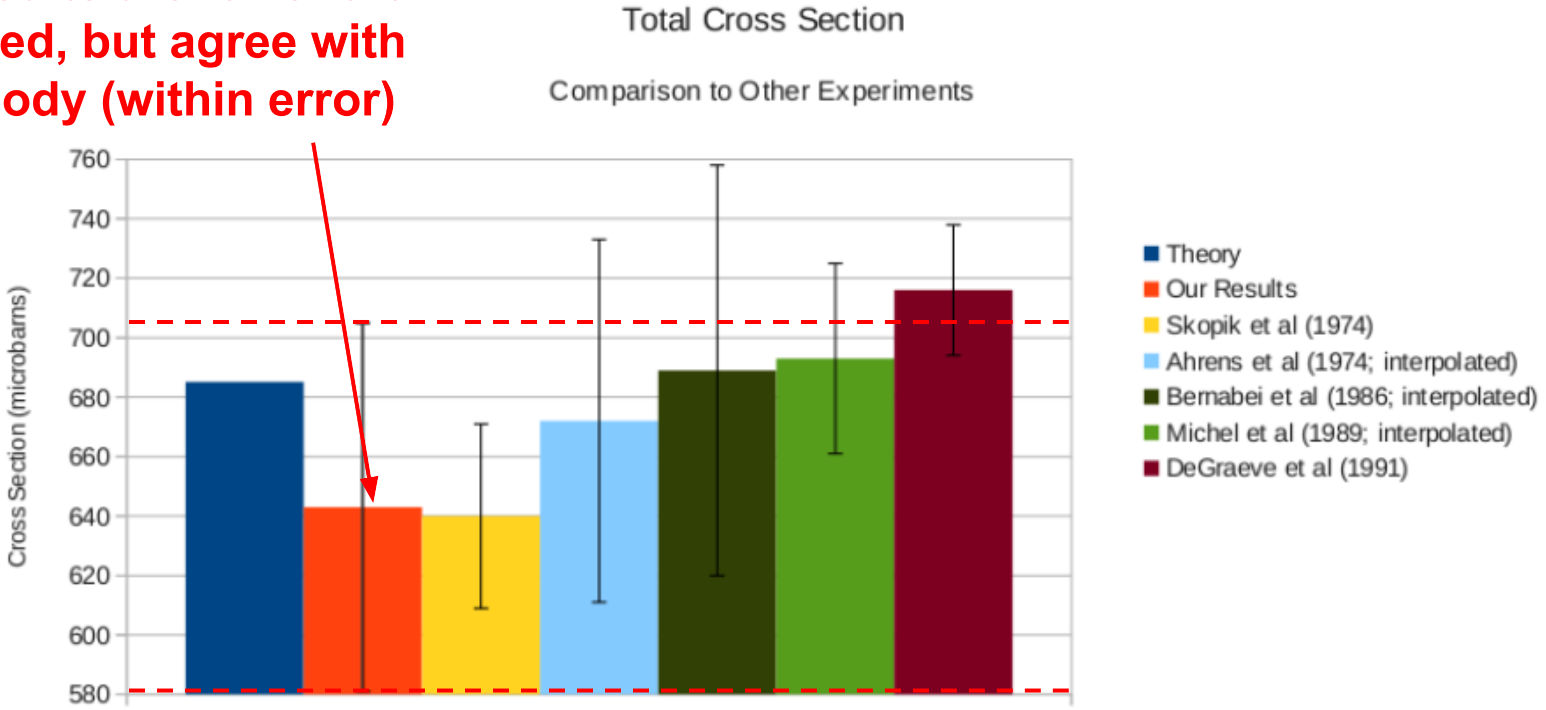

Note: suppressed zero

✓ **Theory**

Results: Parameterization

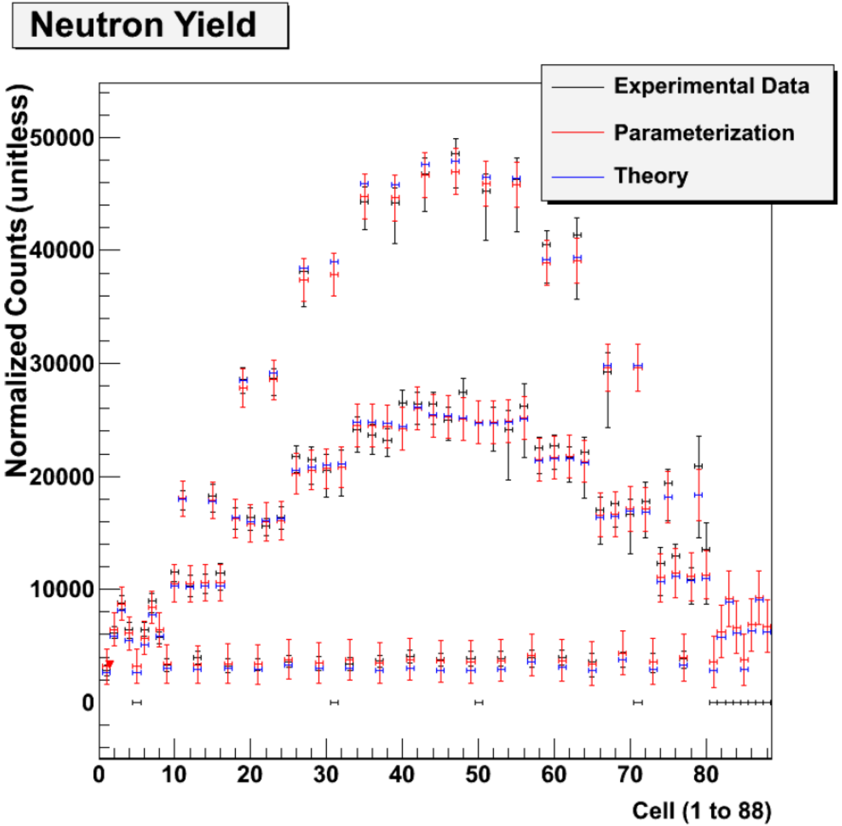

Results: Parameterization

Parameterization fits yield: $X^2_{red.} = 0.31$

Theory fits yield: $X^2_{red.} = 0.74$

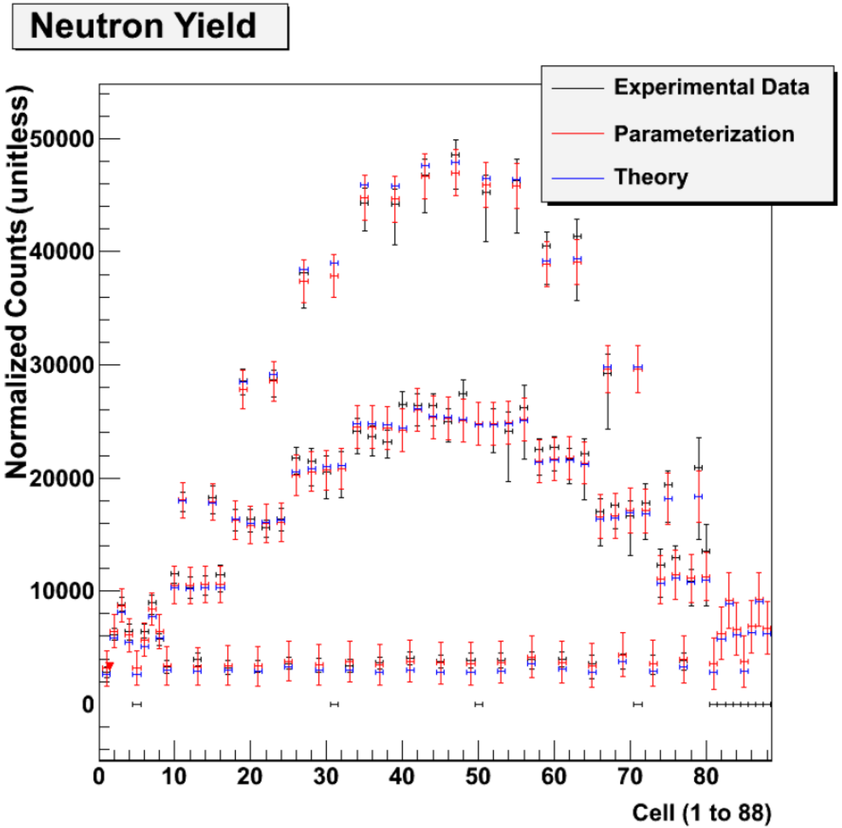

Results: Parameterization

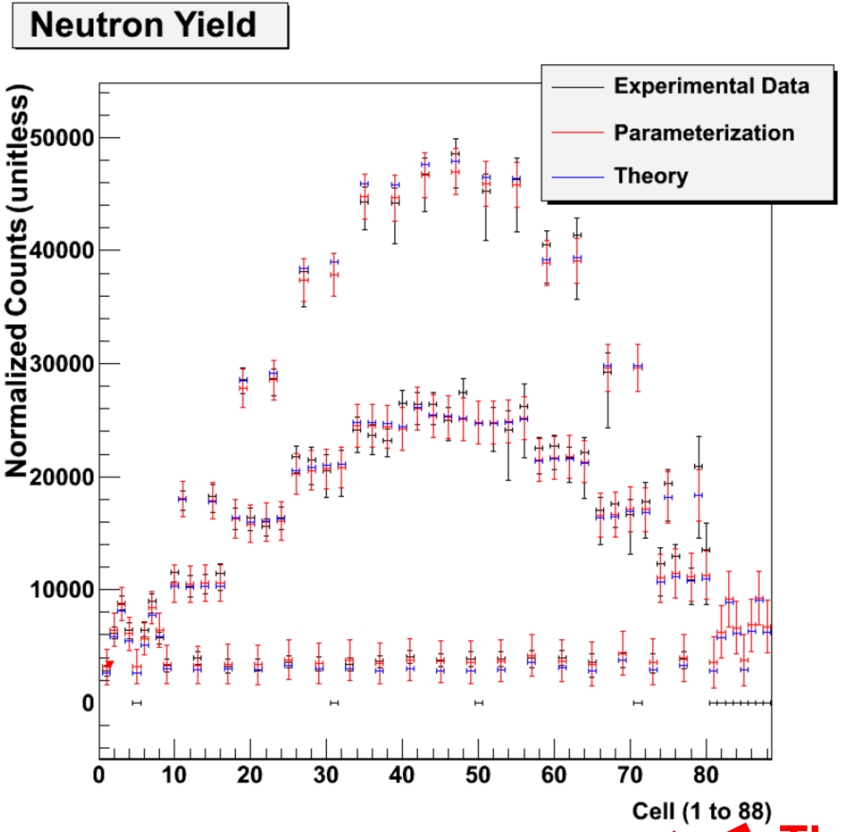

Parameterization fits yield: $X^2_{red.} = 0.31$

Theory fits yield: $X^2_{red.} = 0.74$

✓ Theory

Results: Parameterization

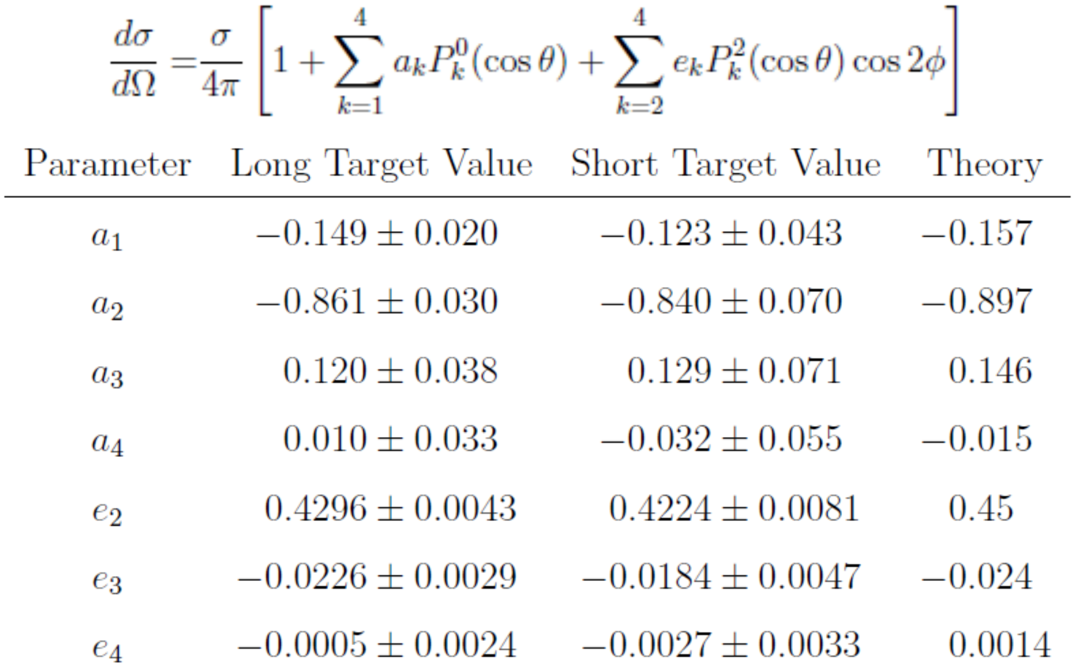

$$\frac{d\sigma}{d\Omega} = \frac{\sigma}{4\pi}\left[1 + \sum_{k=1}^{4} a_k P_k^0(\cos\theta) + \sum_{k=2}^{4} e_k P_k^2(\cos\theta)\cos 2\phi\right]$$

Parameter	Long Target Value	Short Target Value	Theory
a_1	-0.149 ± 0.020	-0.123 ± 0.043	-0.157
a_2	-0.861 ± 0.030	-0.840 ± 0.070	-0.897
a_3	0.120 ± 0.038	0.129 ± 0.071	0.146
a_4	0.010 ± 0.033	-0.032 ± 0.055	-0.015
e_2	0.4296 ± 0.0043	0.4224 ± 0.0081	0.45
e_3	-0.0226 ± 0.0029	-0.0184 ± 0.0047	-0.024
e_4	-0.0005 ± 0.0024	-0.0027 ± 0.0033	0.0014

Results: Parameterization

$$\frac{d\sigma}{d\Omega} = \frac{\sigma}{4\pi}\left[1+\sum_{k=1}^{4} a_k P_k^0(\cos\theta) + \sum_{k=2}^{4} e_k P_k^2(\cos\theta)\cos 2\phi\right]$$

Parameter	Long Target Value	Short Target Value	Theory	
a_1	-0.149 ± 0.020	-0.123 ± 0.043	-0.157	✓
a_2	-0.861 ± 0.030	-0.840 ± 0.070	-0.897	✗
a_3	0.120 ± 0.038	0.129 ± 0.071	0.146	✓
a_4	0.010 ± 0.033	-0.032 ± 0.055	-0.015	**Could be 0**
e_2	0.4296 ± 0.0043	0.4224 ± 0.0081	0.45	✗
e_3	-0.0226 ± 0.0029	-0.0184 ± 0.0047	-0.024	✓
e_4	-0.0005 ± 0.0024	-0.0027 ± 0.0033	0.0014	**Could be 0**

Results: Parameterization

$$\frac{d\sigma}{d\Omega} = \frac{\sigma}{4\pi}\left[1+\sum_{k=1}^{4} a_k P_k^0(\cos\theta) + \sum_{k=2}^{4} e_k P_k^2(\cos\theta)\cos 2\phi\right]$$

Parameter	Long Target Value	Short Target Value	Theory
a_1	-0.149 ± 0.020	-0.123 ± 0.043	-0.157 ✓
a_2	-0.861 ± 0.030	-0.840 ± 0.070	-0.897 ✗
a_3	0.120 ± 0.038	0.129 ± 0.071	0.146 ✓
a_4	0.010 ± 0.033	-0.032 ± 0.055	-0.015 **Could be 0**
e_2	0.4296 ± 0.0043	0.4224 ± 0.0081	0.45 ✗
e_3	-0.0226 ± 0.0029	-0.0184 ± 0.0047	-0.024 ✓
e_4	-0.0005 ± 0.0024	-0.0027 ± 0.0033	0.0014 **Could be 0**

Larger than theory

Smaller than theory

Negative covariance?

Results: Parameterization

Correlation matrix

Parameter	a_1	a_2	a_3	a_4	e_2	e_3	e_4
a_1	1	0.65	0.30	0.40	-0.36	0.41	0.19
a_2	0.65	1	0.72	0.60	-0.61	-0.12	0.38
a_3	0.30	0.72	1	0.67	-0.46	-0.52	0.59
a_4	0.40	0.60	0.67	1	-0.40	-0.19	0.39
e_2	-0.36	-0.61	-0.46	-0.40	1	0.18	-0.24
e_3	0.41	-0.12	-0.52	-0.19	0.18	1	-0.23
e_4	0.19	0.38	0.59	0.39	-0.24	-0.23	1

Results: Parameterization

Negative correlation explains discrepancy with theory

Correlation matrix

Parameter	a_1	a_2	a_3	a_4	e_2	e_3	e_4
a_1	1	0.65	0.30	0.40	-0.36	0.41	0.19
a_2	0.65	1	0.72	0.60	-0.61	-0.12	0.38
a_3	0.30	0.72	1	0.67	-0.46	-0.52	0.59
a_4	0.40	0.60	0.67	1	-0.40	-0.19	0.39
e_2	-0.36	-0.61	-0.46	-0.40	1	0.18	-0.24
e_3	0.41	-0.12	-0.52	-0.19	0.18	1	-0.23
e_4	0.19	0.38	0.59	0.39	-0.24	-0.23	1

Results: Parameterization

We expect a strong *physical* correlation between a_2 and e_2:

$a_2 \; \alpha \; |E1|^2 + |M1|^2 + \ldots$

$e_2 \; \alpha \; |E1|^2 - |M1|^2 + \ldots$

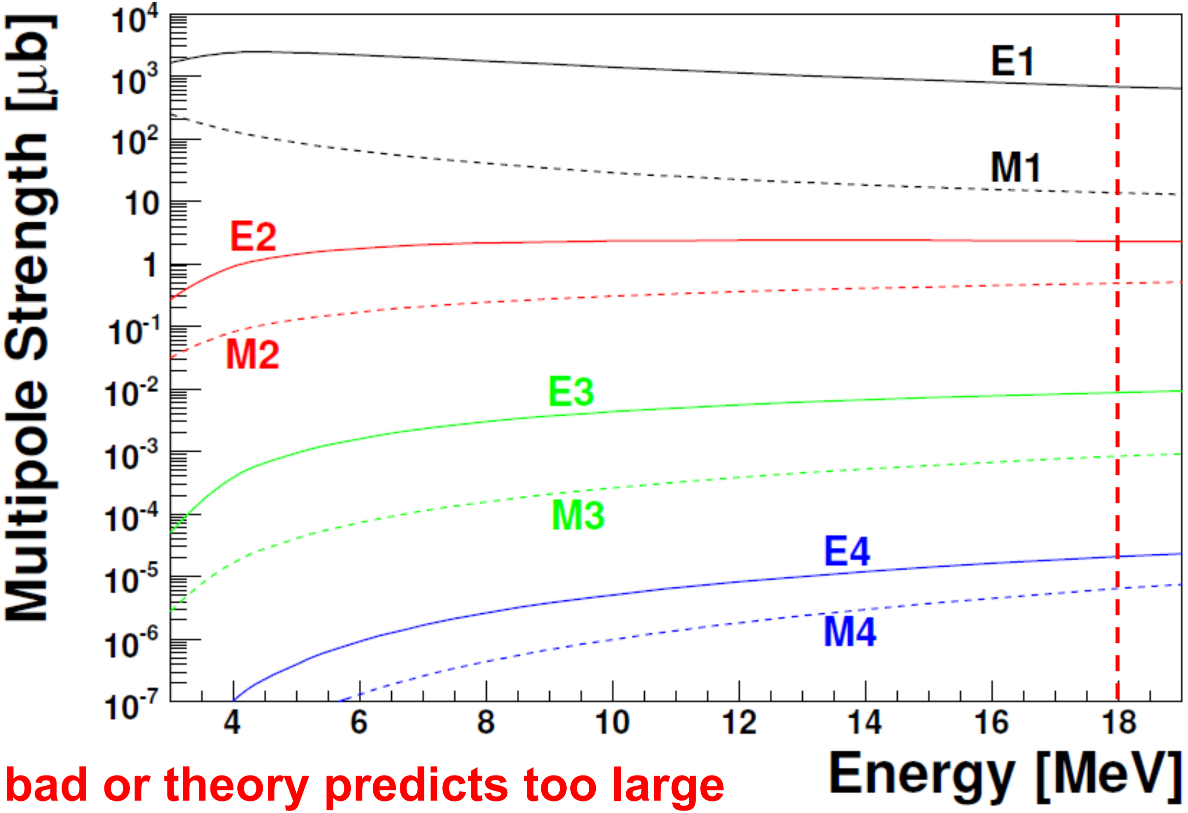

Image credit: Blackston (2007)

Our parameterization is bad or theory predicts too large of a value for M1.

Results: Parameterization

We expect a strong *physical* correlation between a_2 and e_2:

$a_2 \;\; \alpha \; |E1|^2 + |M1|^2 + \ldots$

$e_2 \;\; \alpha \; |E1|^2 - |M1|^2 + \ldots$

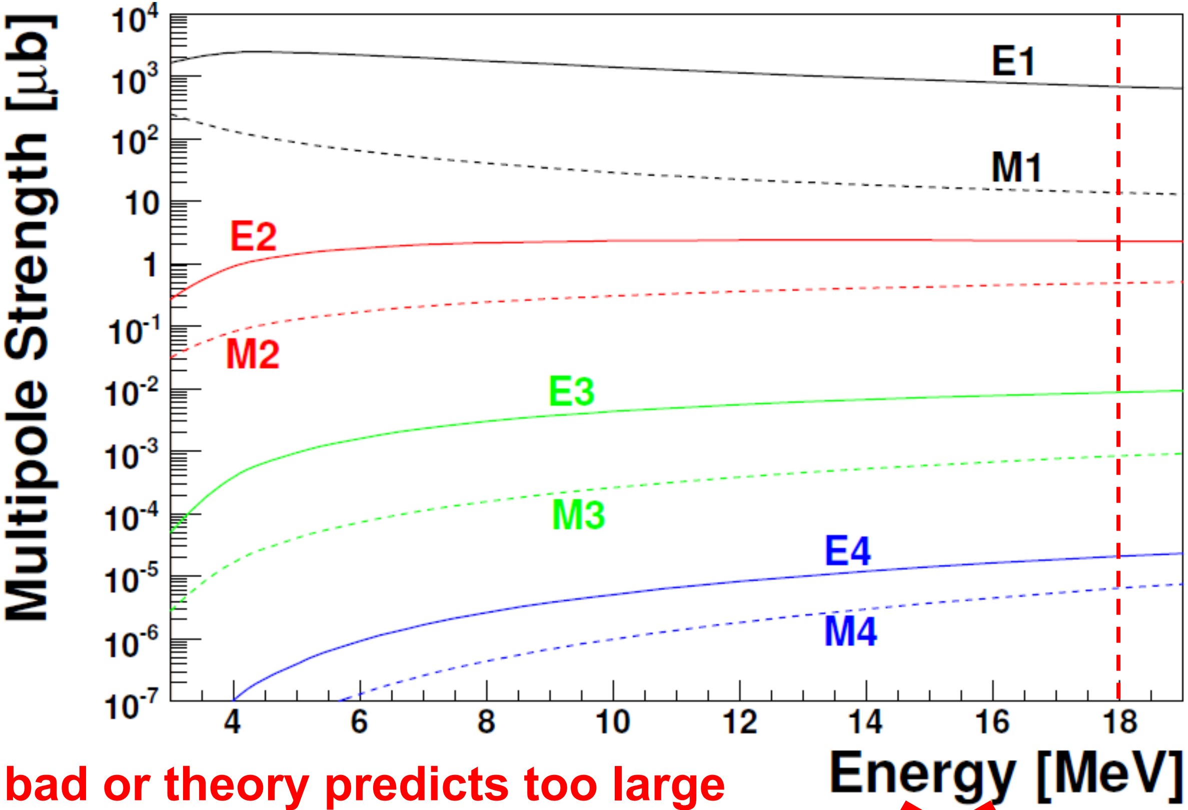

Image credit: Blackston (2007)

Our parameterization is bad or theory predicts too large of a value for M1.

Results: Parameterization

We can calculate observables from the parameterization...

Results: φ-averaged Differential Cross Section

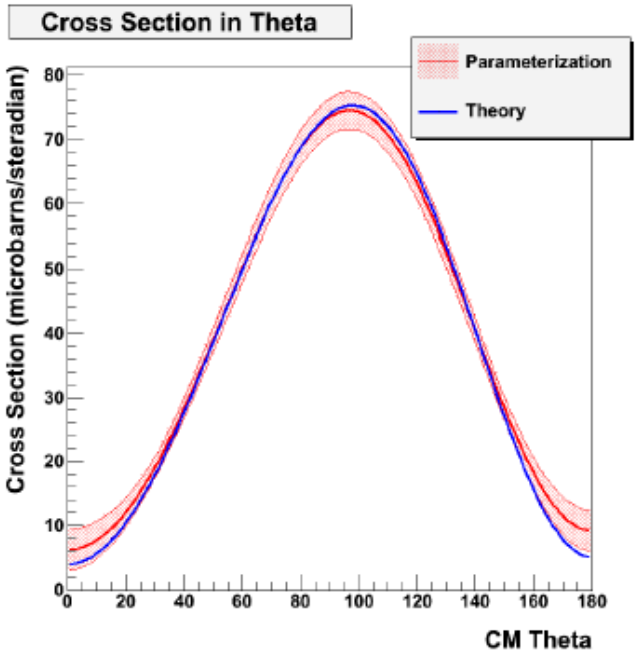

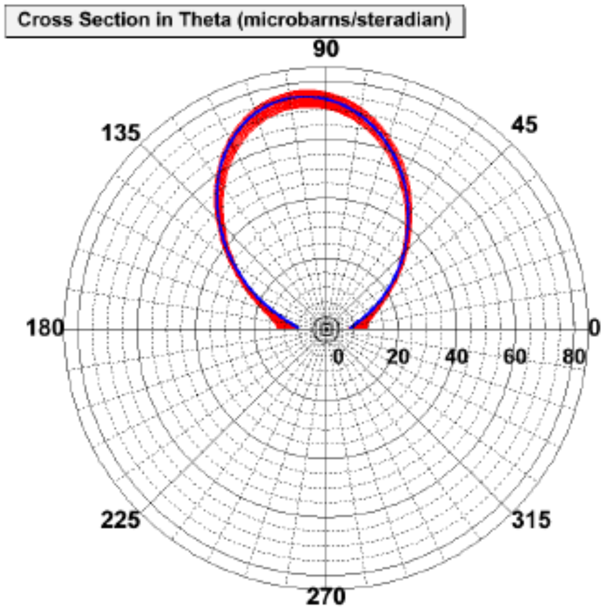

Note: this is an interpolation/extrapolation from the parameterization!

Results: φ-averaged Differential Cross Section

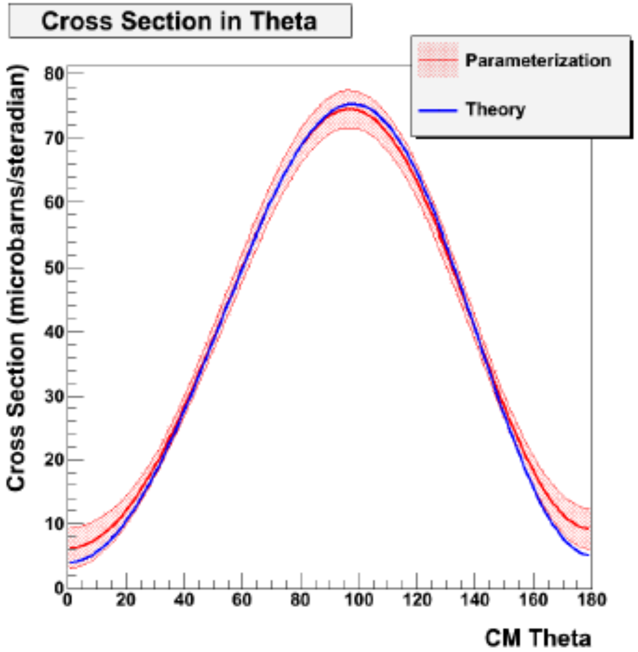

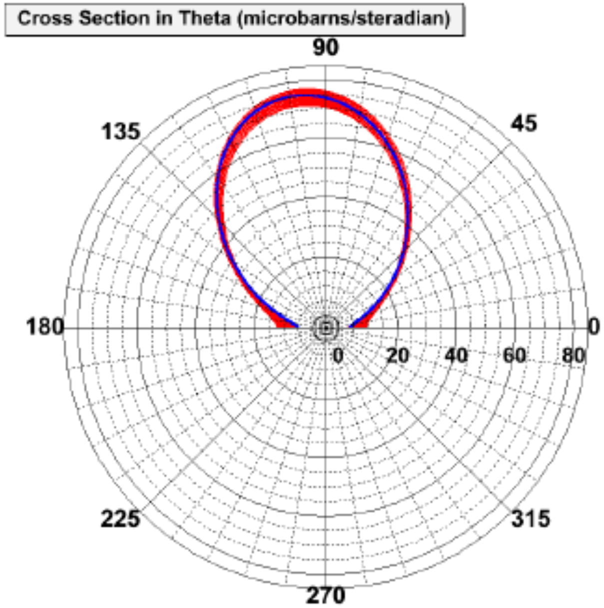

Note: this is an interpolation/extrapolation from the parameterization!

✓ **Theory**

Results: Analyzing Power

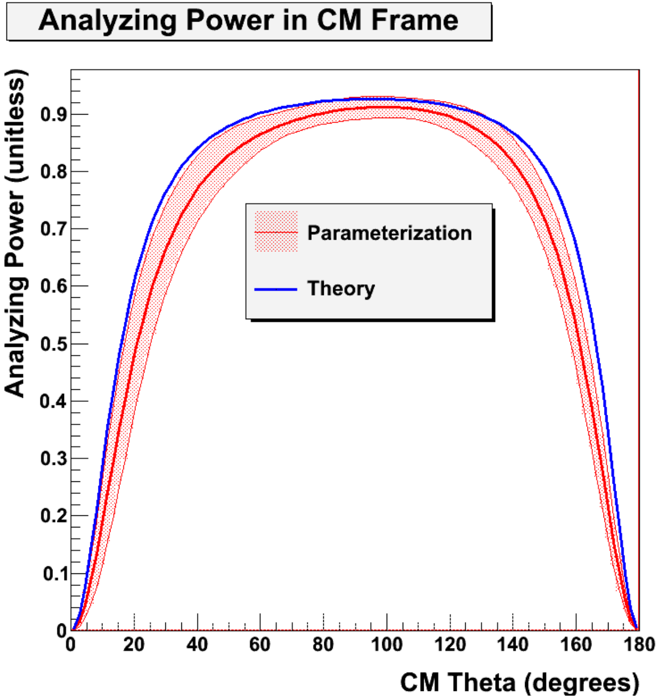

Analyzing Power in CM Frame

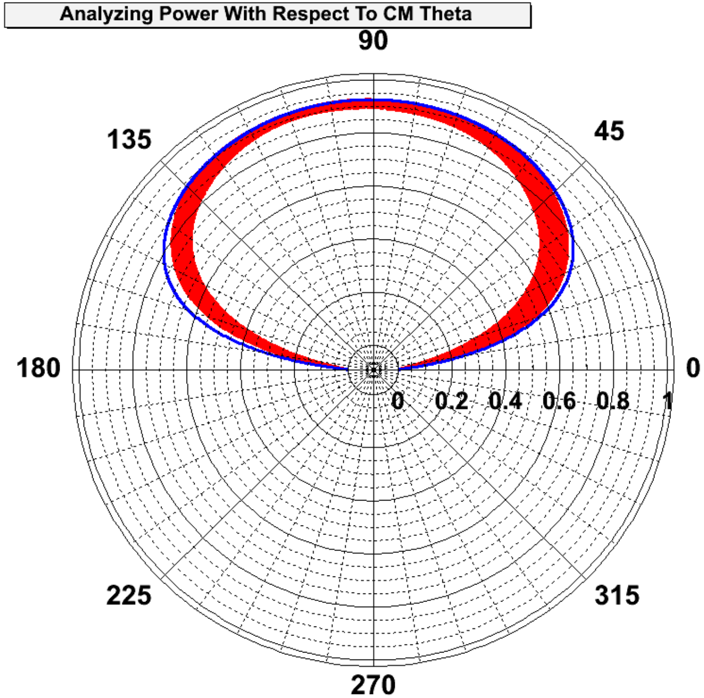

Analyzing Power With Respect To CM Theta

Note: this is an interpolation/extrapolation from the parameterization!

Results: Analyzing Power

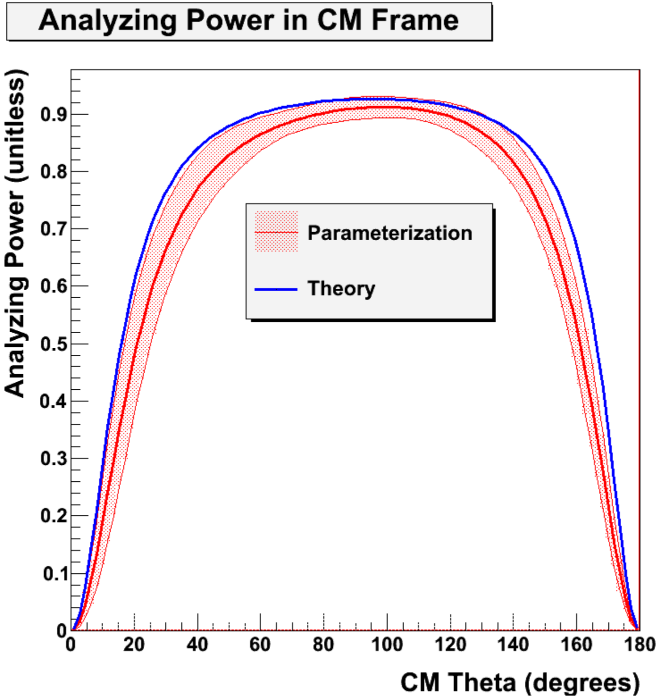

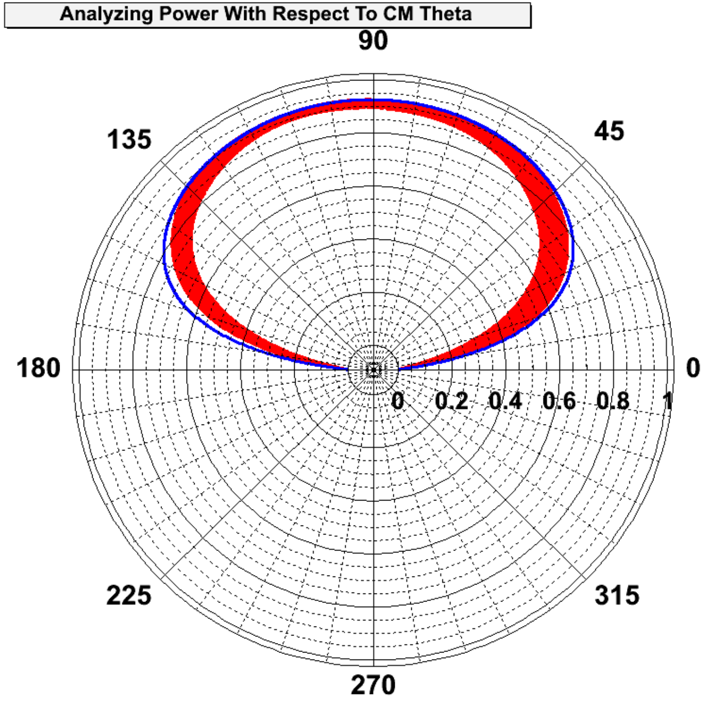

Note: this is an interpolation/extrapolation from the parameterization!

✗ Theory

Results: Analyzing Power

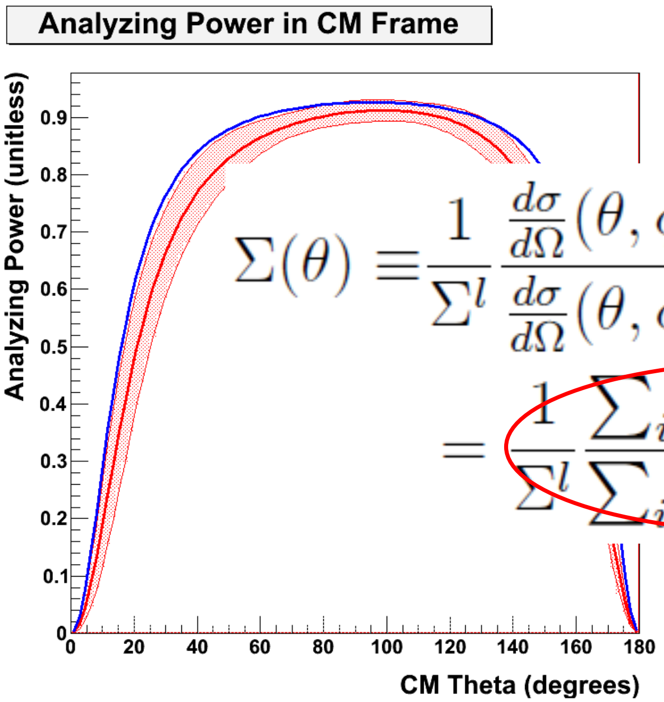

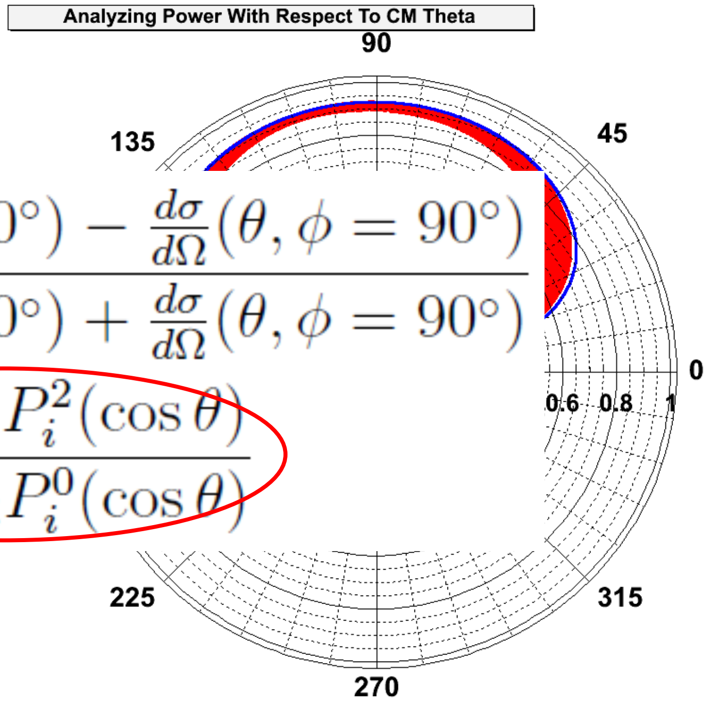

$$\Sigma(\theta) \equiv \frac{1}{\Sigma^l}\frac{\frac{d\sigma}{d\Omega}(\theta,\phi=0^\circ)-\frac{d\sigma}{d\Omega}(\theta,\phi=90^\circ)}{\frac{d\sigma}{d\Omega}(\theta,\phi=0^\circ)+\frac{d\sigma}{d\Omega}(\theta,\phi=90^\circ)}$$

$$= \frac{1}{\Sigma^l}\frac{\sum_{i=2} e_i P_i^2(\cos\theta)}{\sum_{i=1} a_i P_i^0(\cos\theta)}$$

Note: this is an interpolation/extrapolation from the parameterization!

✕ Theory

Results: Differential Cross Section

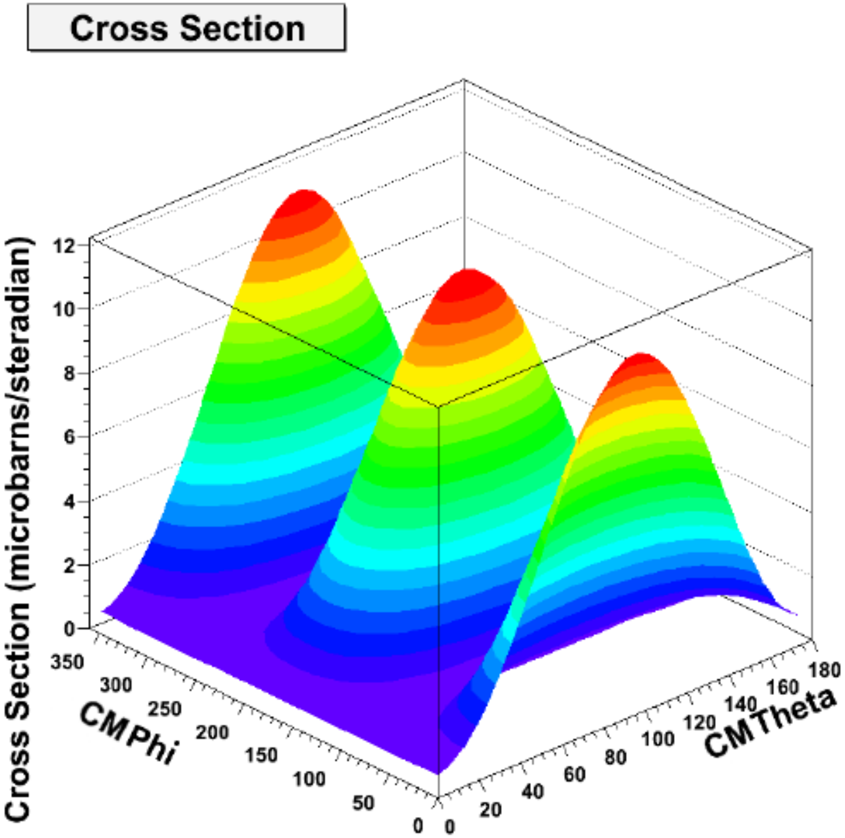

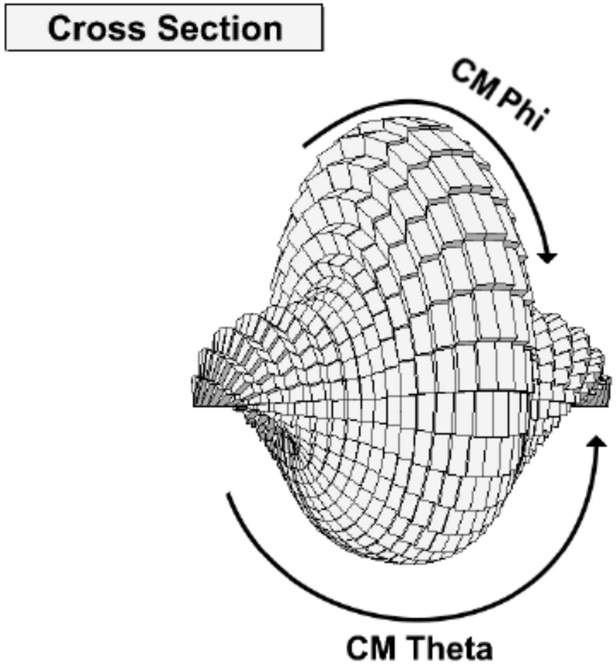

Discussion

Total cross section agrees with theory and previous experiments, but might be systematically low (~7%).

Neutron yield agrees well with theory.

Parameterization agrees with theory and yield, but the a_2 and e_2 parameters don’t agree with theory.

It is unclear whether the a_2/e_2 covariance is physical or an artifact of the analysis: if it is physical, then the theoretical M1 amplitude is likely too large.

Outline

1. Introduction
2. Background
3. Experimental Setup
4. Analysis Methodology
5. Results and Discussion
6. Conclusion ⬅

Conclusion

We report the total cross section (σ), and parameterized differential cross section($d\sigma/d\Omega(\theta,\varphi)$) in terms of associated Legendre polynomials.

Our results agree well with the theoretical prediction except for the values of the a_2 and e_2 parameters.

The theoretical M1 transition amplitude may be too large relative to the other transitions, consistent with the data at 14 and 16 MeV (Blackston, 2007).

Acknowledgements

Dr. Robert Pywell (supervisor) and the rest of the Blowfish Collaboration.

UNIVERSITY OF
SASKATCHEWAN

NSERC
CRSNG

Extra Slides

Introduction: What?

Image credit: http://copypasterepost.com

Introduction: So What!

The deuteron…

1. Has the most energy per nucleon of any nucleus; millions of times more energy-dense than conventional chemicals (MeV vs eV).
2. Can be used in fission bombs and reactors.
3. May be useful for low energy nuclear reactions (i.e. “cold fusion”).
4. Keeps Greg busy.

Background: Previous Experiments

Total Cross Section

(at 18 MeV)

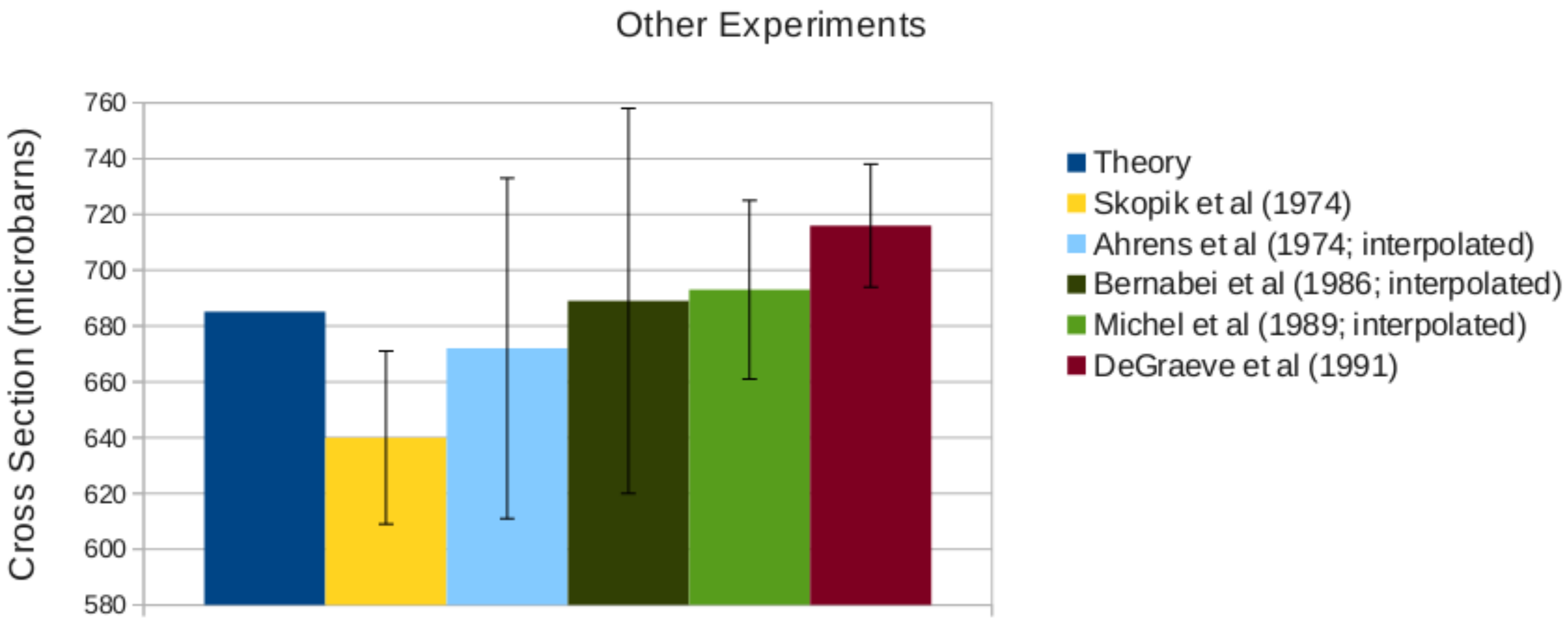

Background: Previous Experiments

Total Cross Section

(at 18 MeV)

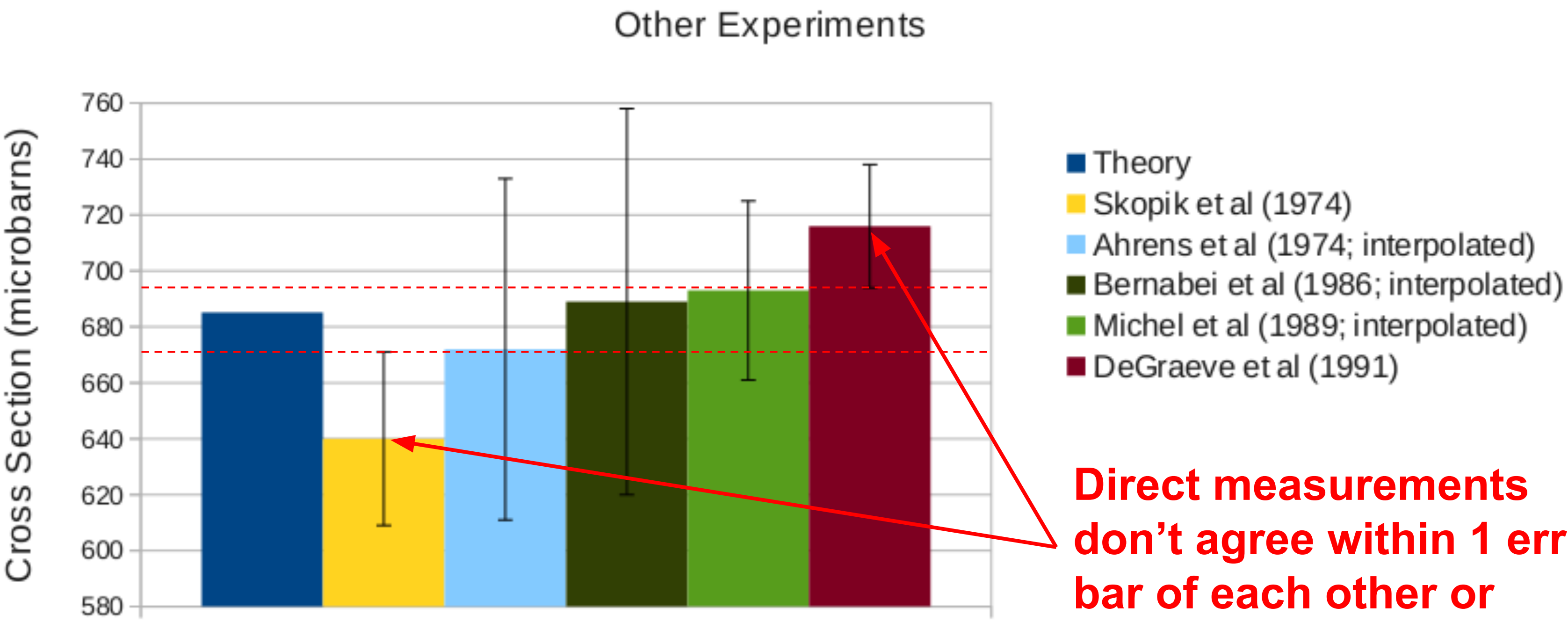

Direct measurements don’t agree within 1 error bar of each other or theory

Background: Previous Experiments

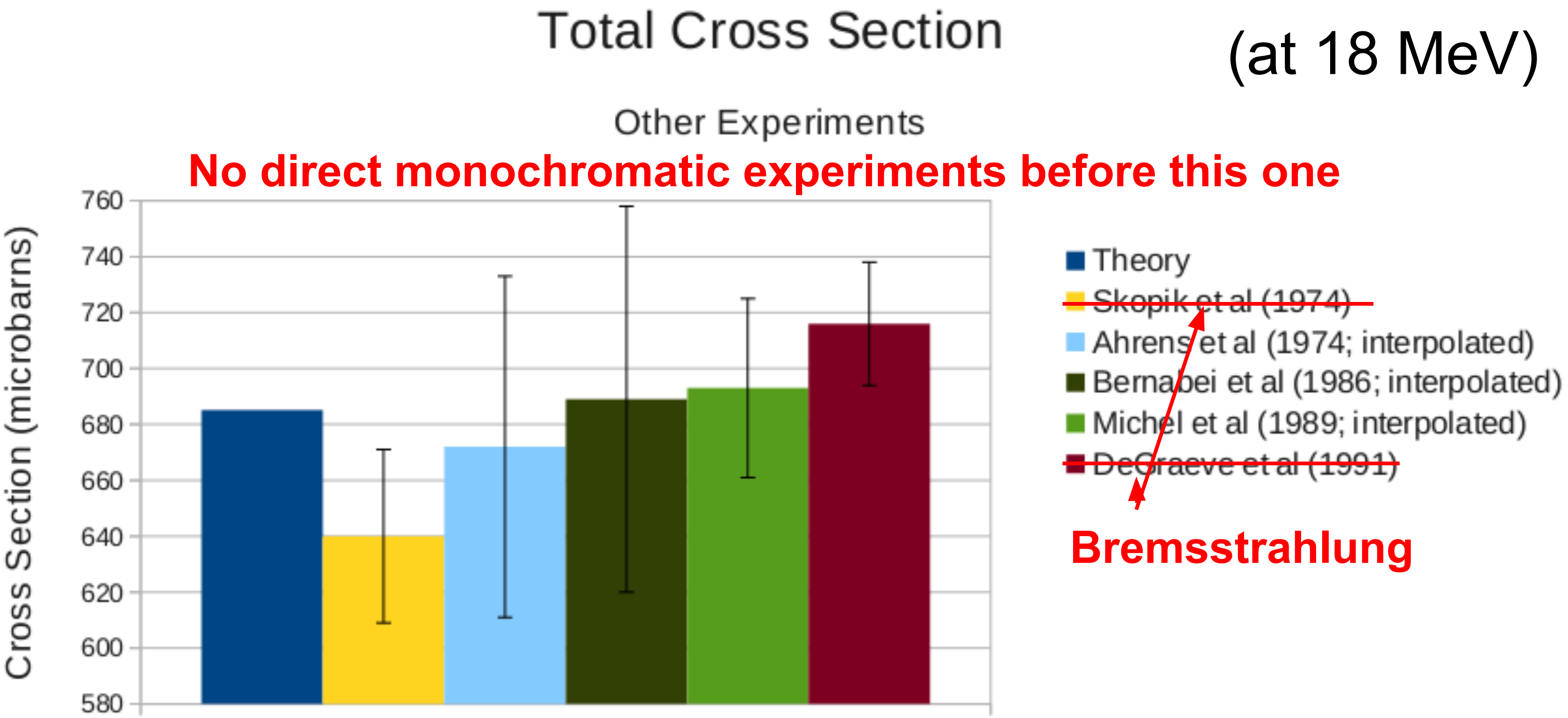

(at 18 MeV)

No direct monochromatic experiments before this one

Bremsstrahlung

Background: Previous Experiments

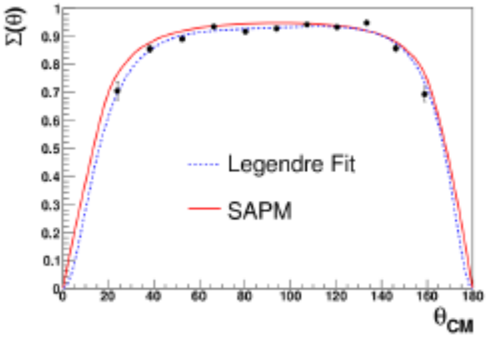

(c) 14 MeV Analyzing Power.

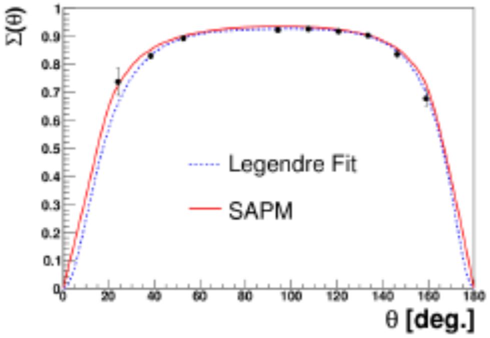

(d) 16 MeV Analyzing Power.

Background: Previous Experiments

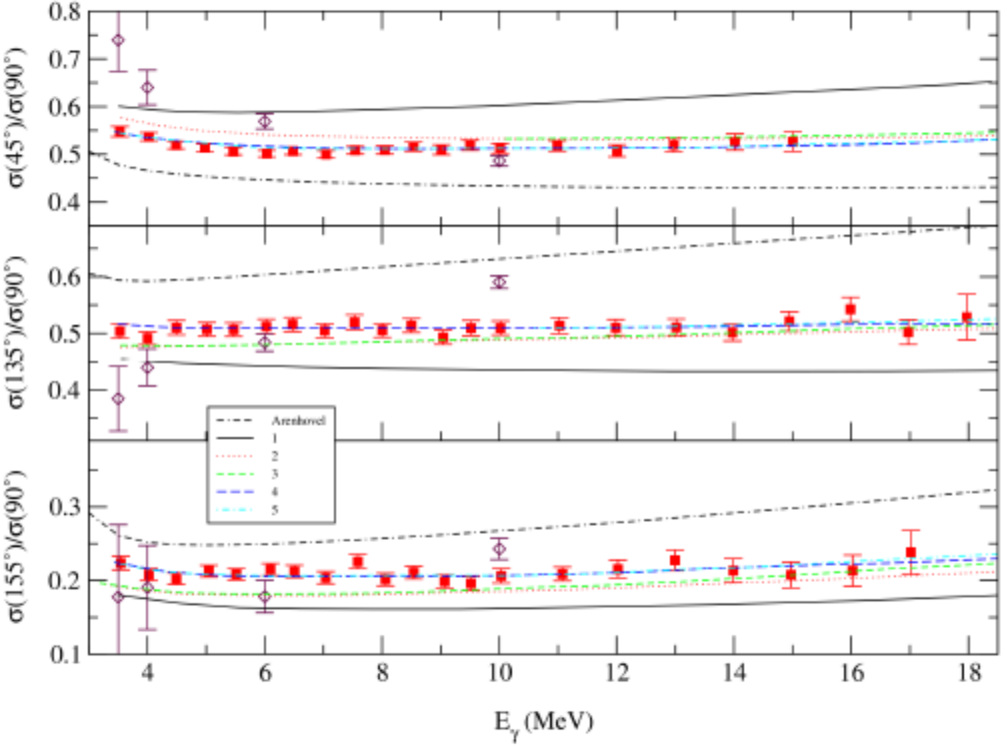

Image credit: Sawatzky (2005)

Background: Previous Experiments

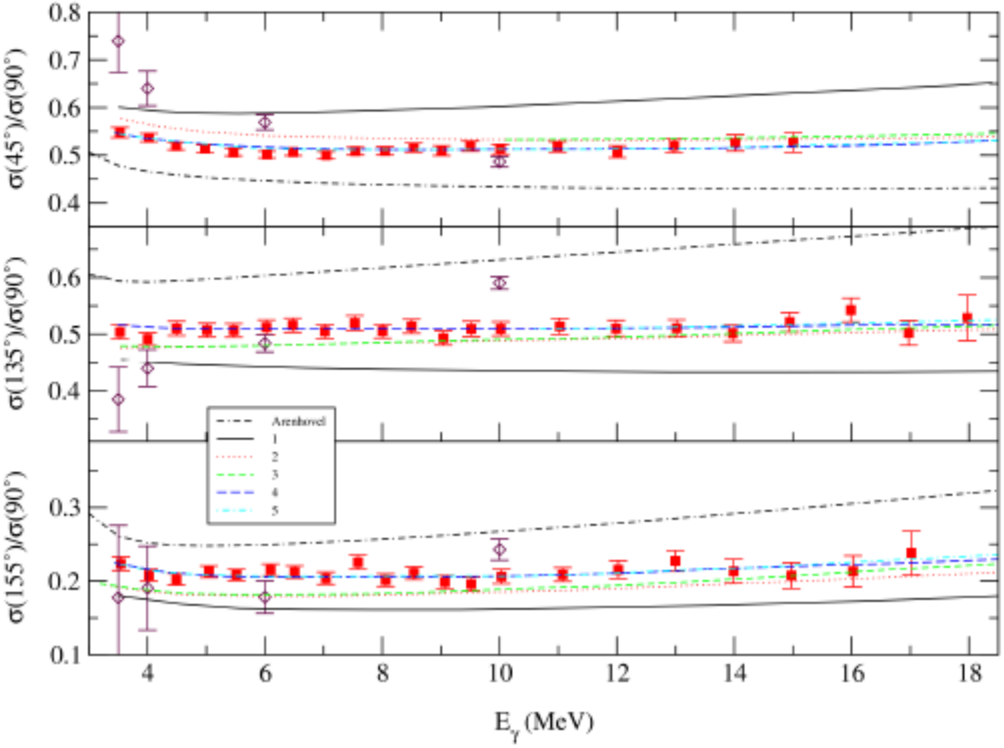

Image credit: Sawatzky (2005)

Background: Previous Experiments

Red data points are from defunct experiment

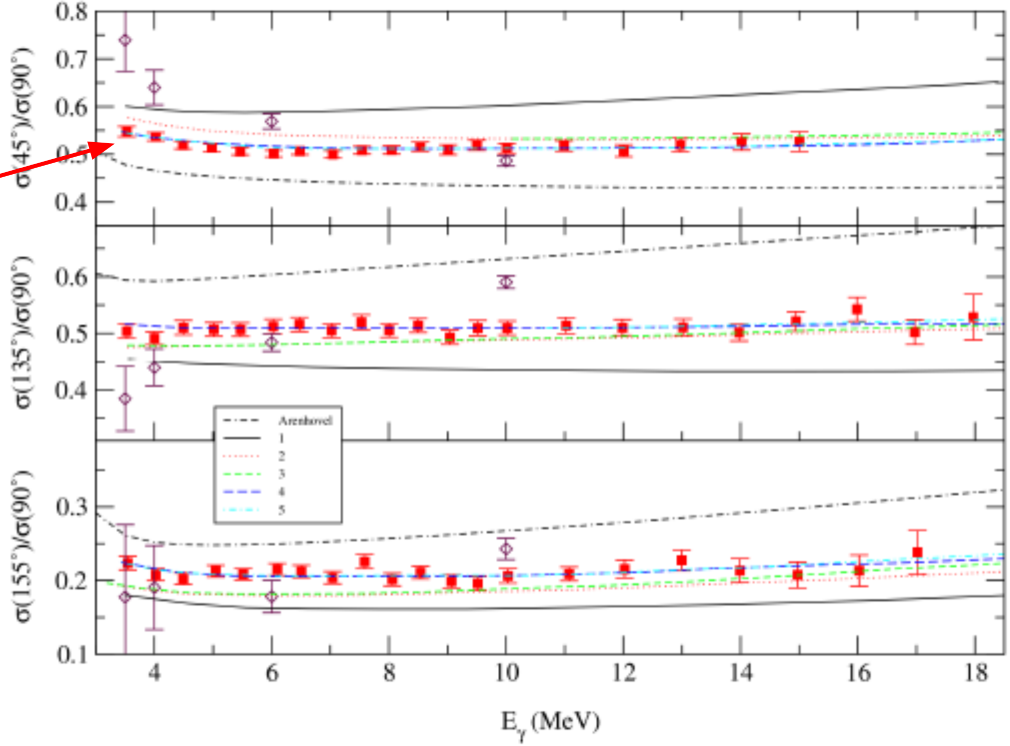

Image credit: Sawatzky (2005)

Background: Previous Experiments

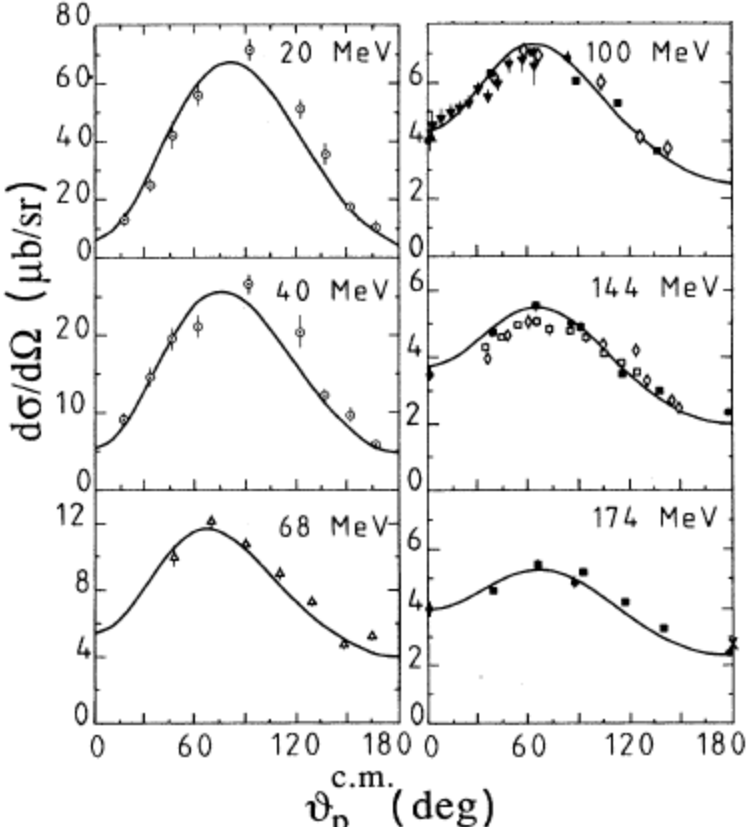

Background: Previous Experiments

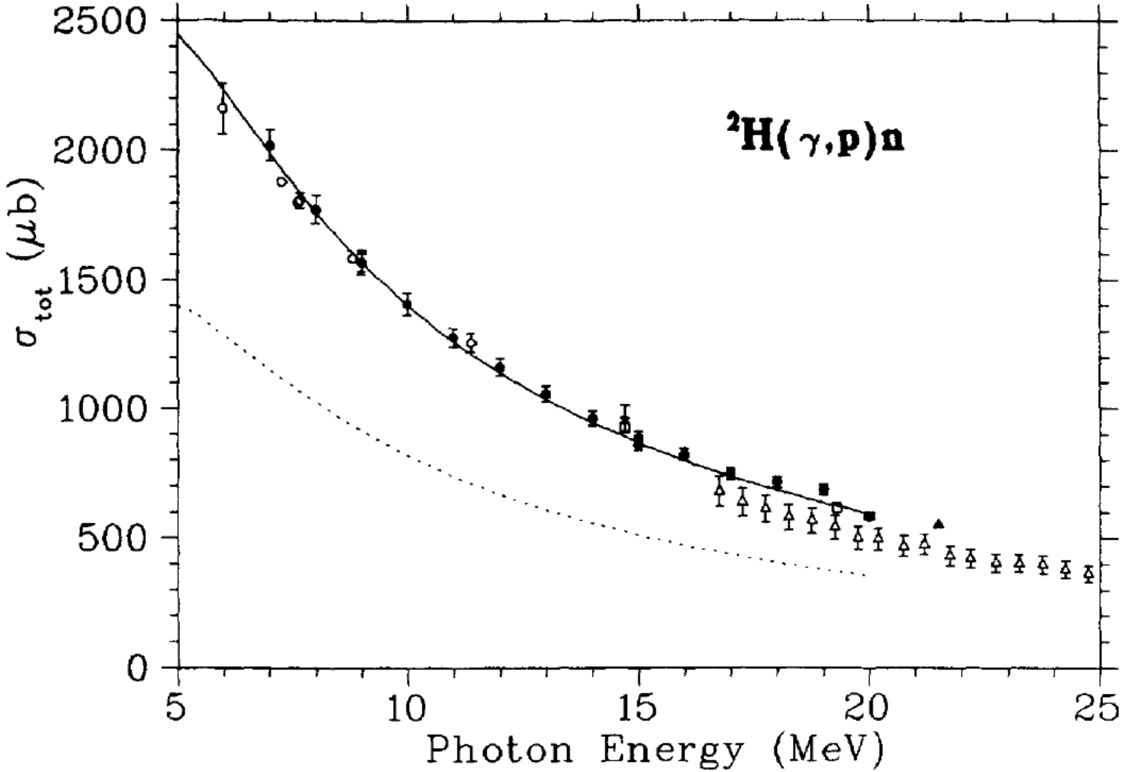

Image credit: De Graeve et al. (1992)

Background: Previous Experiments

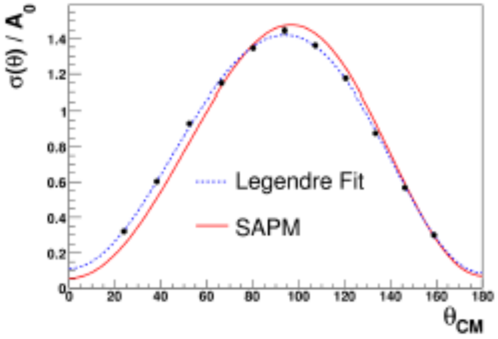

(a) 14 MeV Unpolarized Cross Section.

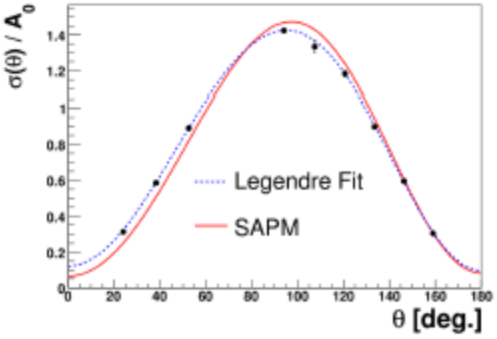

(b) 16 MeV Unpolarized Cross Section.

Image credit: Blackston (2007)

Experimental results from Blowfish for the same reaction (as our current experiment) at 14 and 16 MeV (polarization averaged).

Background: Previous Experiments

Experiment

Theory

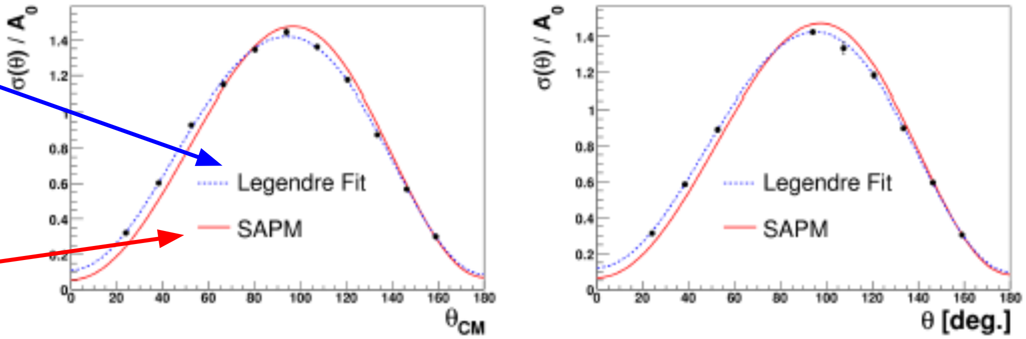

(a) 14 MeV Unpolarized Cross Section.

(b) 16 MeV Unpolarized Cross Section.

Image credit: Blackston (2007)

Experimental results from Blowfish for the same reaction (as our current experiment) at 14 and 16 MeV (polarization averaged).

Background: Previous Experiments

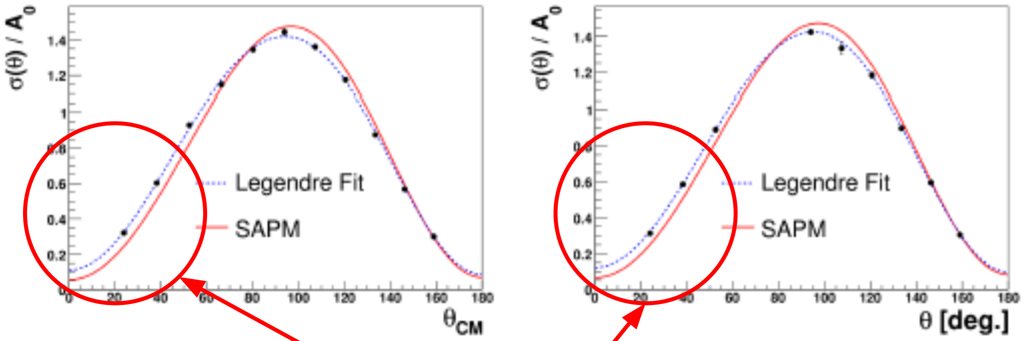

(a) 14 MeV Unpolarized Cross Section.

(b) 16 MeV Unpolarized Cross Section.

Theory underestimates forward angle cross section

Image credit: Blackston (2007)

Background: Previous Experiments

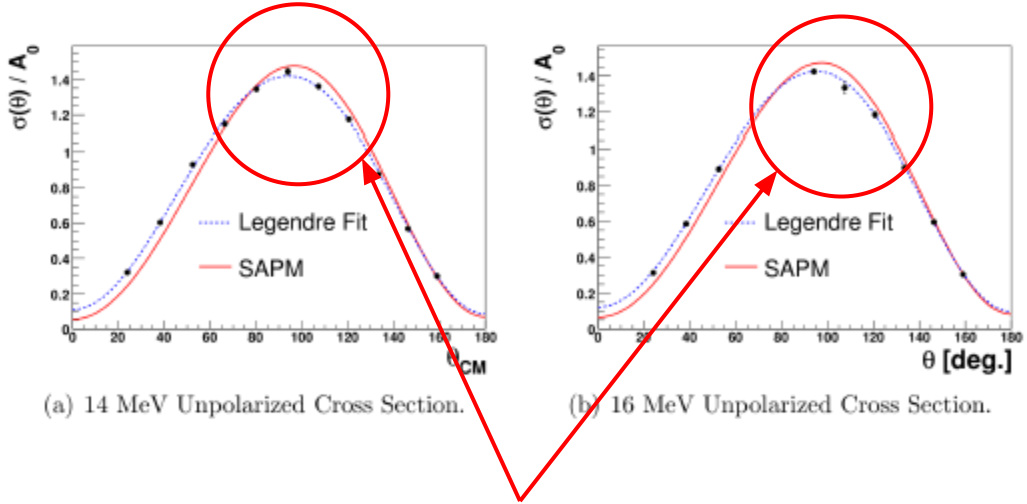

(a) 14 MeV Unpolarized Cross Section.

(b) 16 MeV Unpolarized Cross Section.

Theory overestimates intermediate angle cross section

Image credit: Blackston (2007)

Background: Previous Experiments

Summary

Older experiments (i.e. those using bremsstrahlung) can’t be relied upon and must be replaced.

Low energy (~18 MeV) theoretical predictions look good, but high precision results may find a discrepancy: especially at extreme angles.

Background: Meson Exchange

“...if one writes down the most general possible Lagrangian, including all terms consistent with assumed symmetry principles, and then calculates the matrix elements with this Lagrangian to any given order of perturbation theory, the result will simply be the most general possible S matrix consistent with analyticity, perturbative unitarity, cluster decomposition, and the assumed symmetry principles.”

Background: Meson Exchange

Which mesons can be exchanged?

All of them e.g. π, ω, δ, and ρ. At least one meson per type (charged/uncharged and scalar/vector) is necessary to fully account for the QCD degrees of freedom.

There are four unique Lagrangians: one for each type.

Background: The Calculation

All of the observables are calculated from the differential cross section (dσ/dΩ (θ,φ)).

The differential cross section is calculated from the T matrix using:

$$\left(\frac{d\sigma}{d\Omega}\right)_{CM} = \left(\frac{1}{8\pi}\right)^2 \frac{|T_{fi}|^2}{E_{CM}^2} \frac{p^L}{E_\gamma^L}$$

Where the T matrix is defined by:

$$\hat{S}_{fi} = \langle f|i\rangle + (2\pi)^4 i\delta^{(4)}(\mathbf{p}_f - \mathbf{p}_i)\hat{T}_{fi}$$

Background: The Calculation

Schwamb and Arenhövel use an effective nucleon current to calculate the T matrix perturbatively:

$$T_{fi} = \sqrt{\frac{\alpha}{2\pi^2}} \langle n, p | \epsilon^{\mu} J_{\mu} | d \rangle$$

Background: The Calculation

Schwamb and Arenhövel use an effective nucleon current to calculate the T matrix perturbatively:

$$T_{fi} = \sqrt{\frac{\alpha}{2\pi^2}} \langle n, p | \epsilon^\mu J_\mu | d \rangle$$

Background: The Calculation

Schwamb and Arenhövel use an effective nucleon current to calculate the T matrix perturbatively:

$$T_{fi} = \sqrt{\frac{\alpha}{2\pi^2}} \langle n, p | \epsilon^{\mu} J_{\mu} | d \rangle$$

...expanding in terms of electric and magnetic multipoles:

$$\epsilon^{\mu}(\lambda) J_{\mu} = -\sqrt{2\pi} \sum_{L,m} \hat{L} (\hat{\mathrm{E}}^{L}_{m} + \lambda \hat{\mathrm{M}}^{L}_{m}) D^{L}_{m\lambda}(R)$$

Background: The Calculation

Schwamb and Arenhövel use an effective nucleon current to calculate the T matrix perturbatively:

$$T_{fi} = \sqrt{\frac{\alpha}{2\pi^2}} \langle n, p | \epsilon^{\mu} J_{\mu} | d \rangle$$

...expanding in terms of electric and magnetic multipoles:

$$\epsilon^{\mu}(\lambda) J_{\mu} = -\sqrt{2\pi} \sum_{L,m} \hat{L} (\hat{\mathrm{E}}^{L}_{m} + \lambda \hat{\mathrm{M}}^{L}_{m}) D^{L}_{m\lambda}(R)$$

Background: The Calculation

The electric and magnetic multipoles are calculated using the electric and magnetic multipole field operators:

$$\hat{\mathrm{M}}^L \equiv \int \hat{j} \cdot \vec{A}^l_m d^3x = \int \hat{j} \cdot [\frac{i^{L-1}}{\sqrt{L(L+1)}}(\vec{r} \times \nabla) j_L \vec{Y}^L_m] d^3x$$

$$\hat{\mathrm{E}}^L \equiv \int \hat{j} \cdot \vec{A}^l_e d^3x = \int \hat{j} \cdot \frac{i}{\omega} \nabla \times \vec{A}^l_m d^3x$$

Background: The Calculation

The electric and magnetic multipoles are calculated using the electric and magnetic multipole field operators:

$$\hat{\mathrm{M}}^L \equiv \int \hat{\jmath} \cdot \vec{A}^l_m d^3x = \int \hat{\jmath} \cdot [\frac{i^{L-1}}{\sqrt{L(L+1)}}(\vec{r} \times \nabla) j_L \vec{Y}^L_m] d^3x$$

$$\hat{\mathrm{E}}^L \equiv \int \hat{\jmath} \cdot \vec{A}^l_e d^3x = \int \hat{\jmath} \cdot \frac{i}{\omega} \nabla \times \vec{A}^l_m d^3x$$

Background: The Calculation

The electric and magnetic multipoles are calculated using the electric and magnetic multipole field operators:

$$\hat{\mathrm{M}}^L \equiv \int \hat{j} \cdot \vec{A}^l_m d^3x = \int \hat{j} \cdot [\frac{i^{L-1}}{\sqrt{L(L+1)}}(\vec{r} \times \nabla) j_L \vec{Y}^L_m] d^3x$$

$$\hat{\mathrm{E}}^L \equiv \int \hat{j} \cdot \vec{A}^l_e d^3x = \int \hat{j} \cdot \frac{i}{\omega} \nabla \times \vec{A}^l_m d^3x$$

Background: Theory

Summary

The nucleon-nucleon potential used was the Elster potential which is based on the phenomenological 1987 Bonn r-potential with corrections to extend it past pion threshold (135 MeV).

The calculation by Schwamb and Arenhövel uses a non-relativistic numerical deuteron with: retarded meson exchange, delta baryon degree-of-freedom, single off-shell meson correction, and relativistic corrections.

Background: Detection Principles

Contain benzene rings

Liquid organic scintillators are able to preserve information about how the energy was deposited in them.

Non-relativistic heavy particles deposit their energy non-linearly, resulting in lots of delayed *fluorescence*.

The length of scintillation time is proportional to the mass of the incident particle.

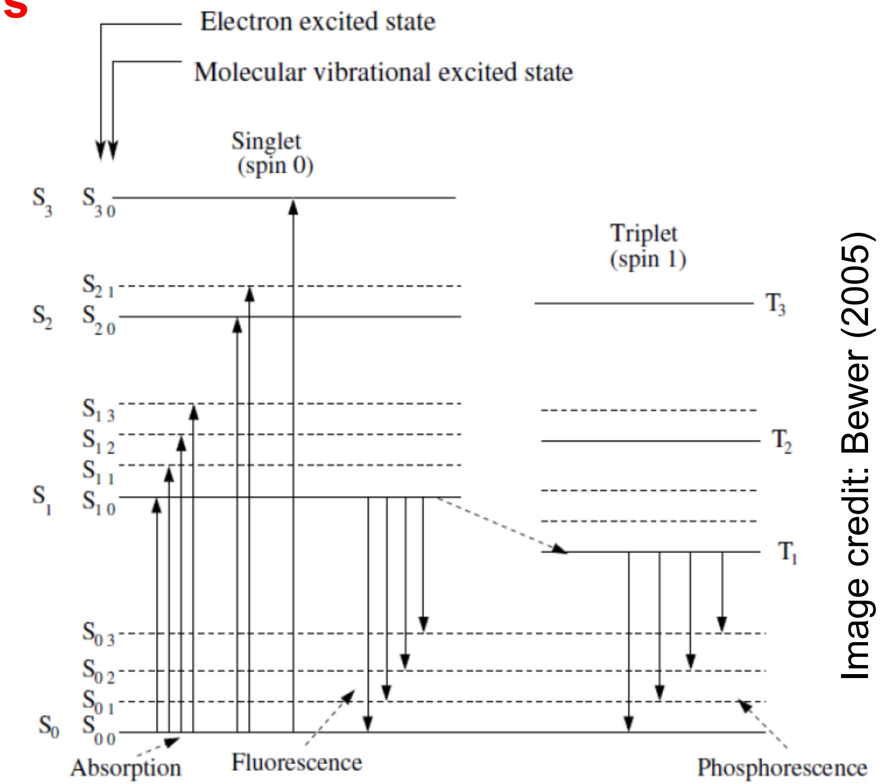

Image credit: Bewer (2005)

Background: Detection Principles

Liquid organic scintillators are able to preserve information about how the energy was deposited in them.

Non-relativistic heavy particles deposit their energy non-linearly, resulting in lots of delayed *fluorescence*.

The length of scintillation time is proportional to the mass of the incident particle.

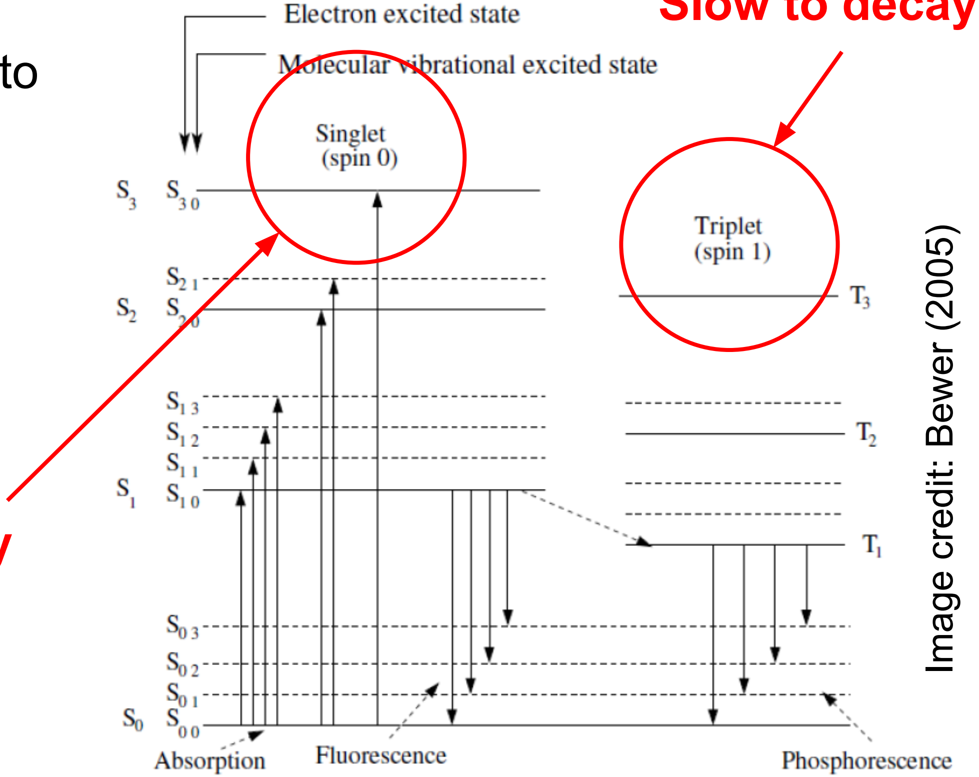

Slow to decay

Quick to decay

Image credit: Bewer (2005)

Background: Detection Principles

Liquid organic scintillators are able to preserve information about how the energy was deposited in them.

Non-relativistic heavy particles deposit their energy non-linearly, resulting in lots of delayed *fluorescence*.

The length of scintillation time is proportional to the mass of the incident particle.

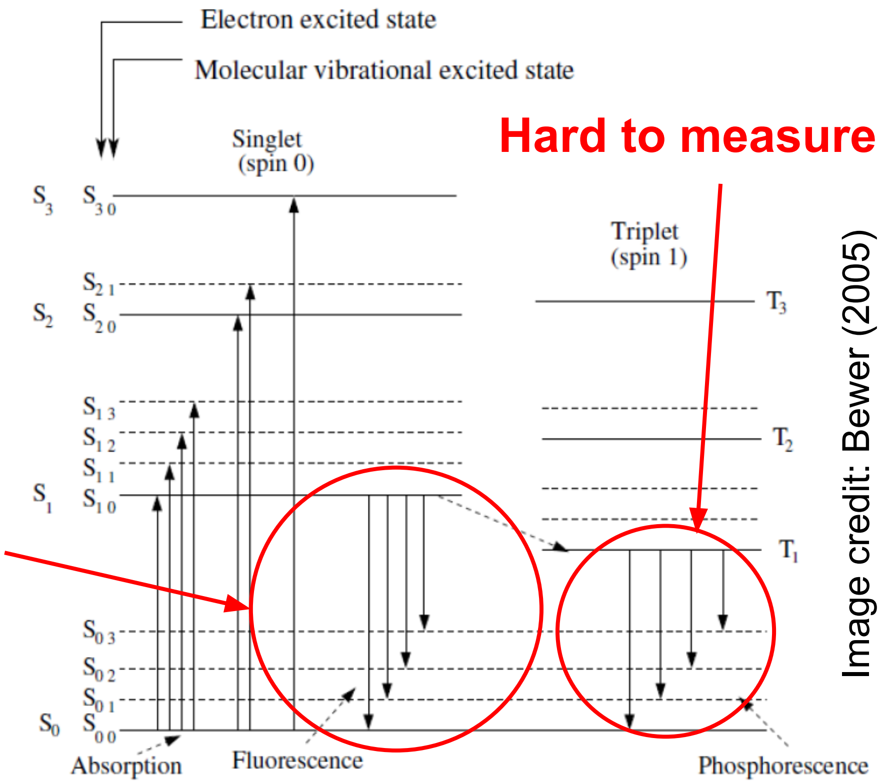

Image credit: Bewer (2005)

Background: Detection Principles

Triplet states are (ideally) only measured if they are excited into singlet states, then radiate: *delayed fluorescence*.

Quicker energy deposition (e.g. heavy particles) leads to more collisions which increases delayed fluorescence.

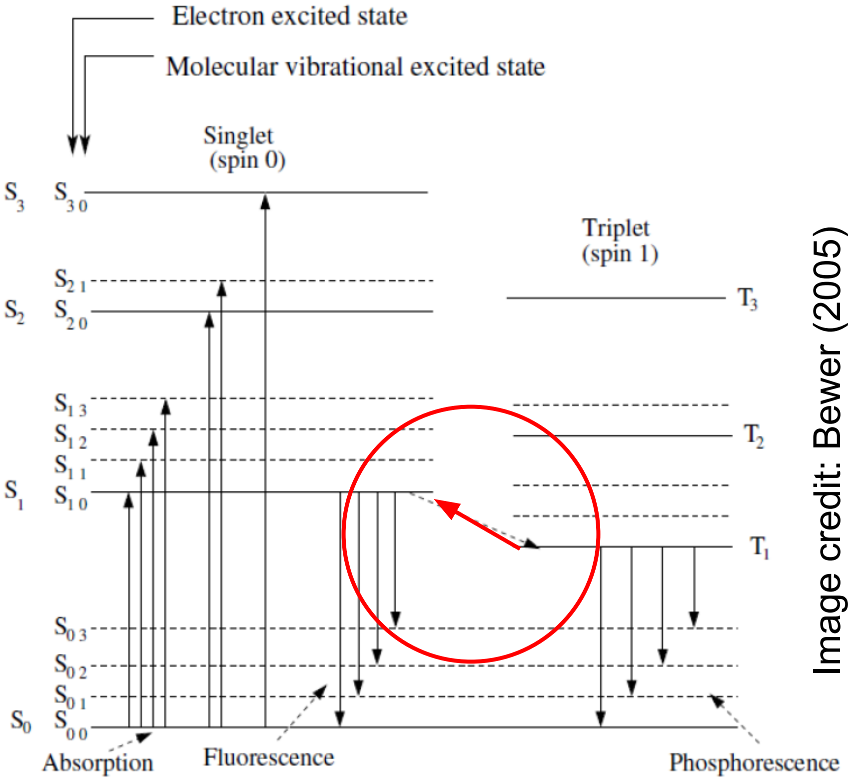

Image credit: Bewer (2005)

Background: Detection Principles

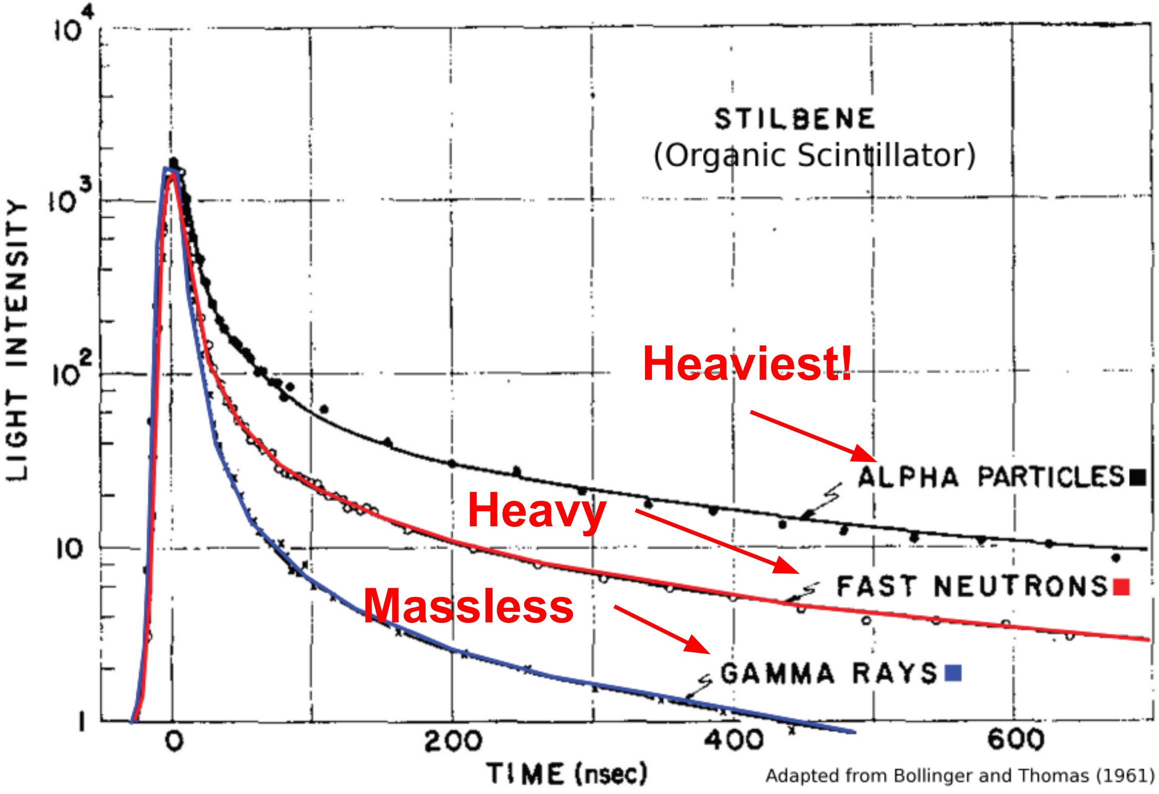

Adapted from Bollinger and Thomas (1961)

Experiment: Beam

HI$\vec{\gamma}$S uses a free-electron laser (FEL) to get high energy photons (up to 95 MeV).

How it works:

http://www.tunl.duke.edu/web.tunl.2011a.higs.php

Analysis: Multiplicity Cut

<u>Multiplicity:</u>

the number of concurrent (within ~ms') events.

<u>Purpose:</u>

eliminate partial events from analysis.

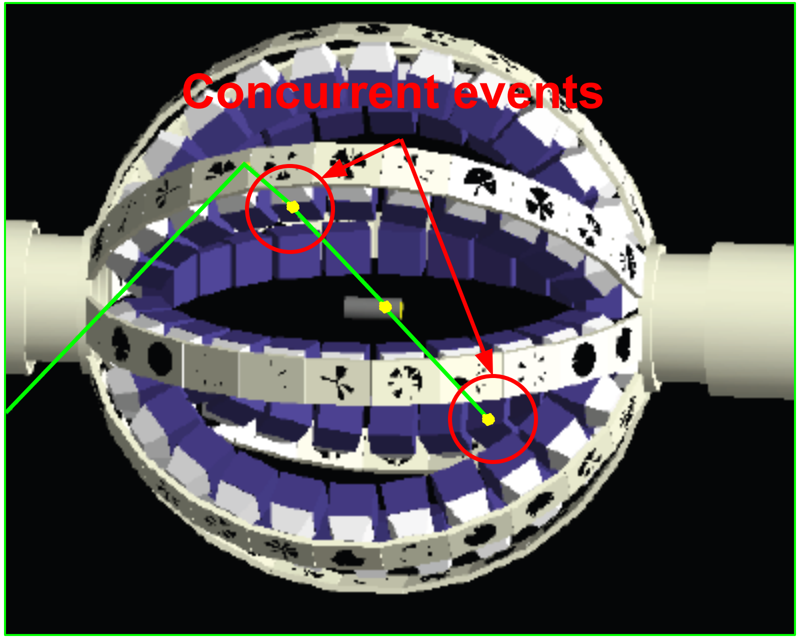

Analysis: Pulse-Shape Discrimination (PSD) Cut

<u>Pulse-shape Discrimination:</u>

utilize liquid organic scintillator’s property to differentiate between measured particle types.

<u>Purpose:</u>

eliminate photons from analysis.

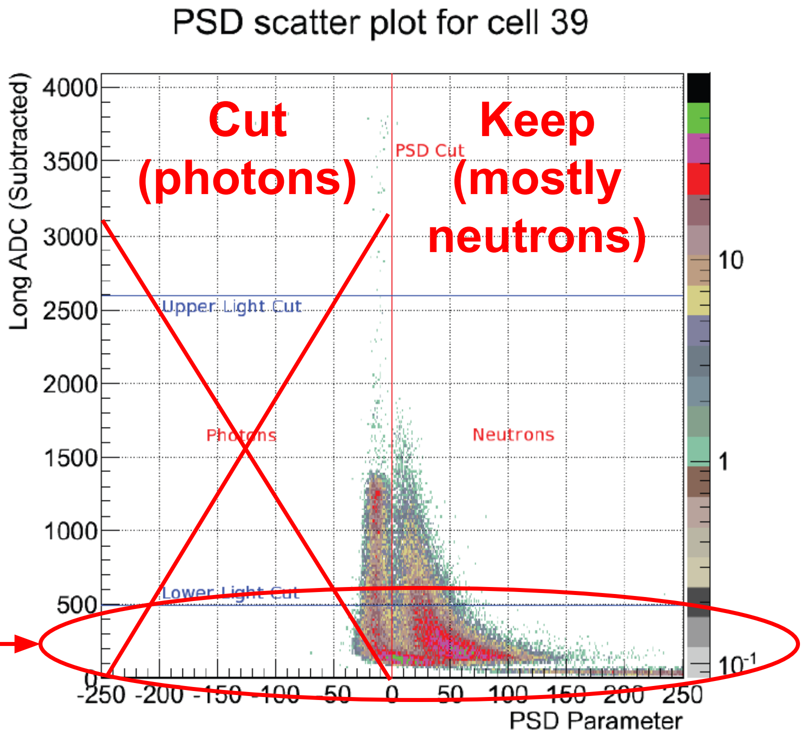

Notice overlap region: we can’t depend on PSD here

Analysis: Energy Cut

Energy (light) cut:

remove all events above or below a detector response in electron-equivalent eV (eVee).

Purpose:

eliminate artifacts of our detectors (high cut) and region of PSD overlap (low cut).

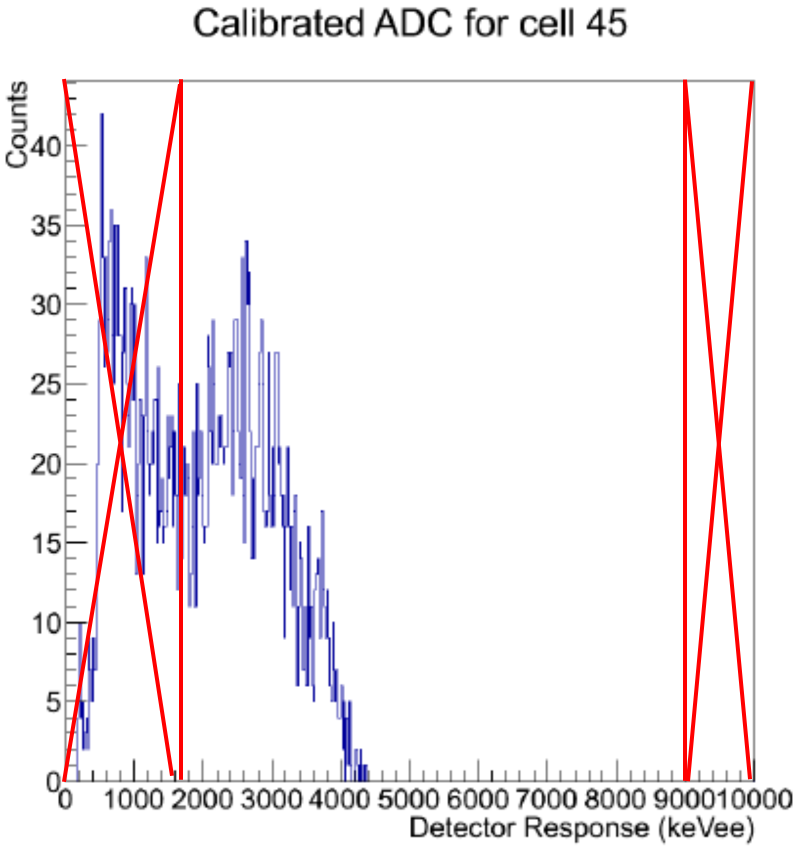

Analysis: Time-of-Flight Cut

Time-of-Flight:

assuming an elastic photodisintegration, we know when the neutrons from our reaction can arrive.

Purpose:

eliminate kinematically prohibited events.

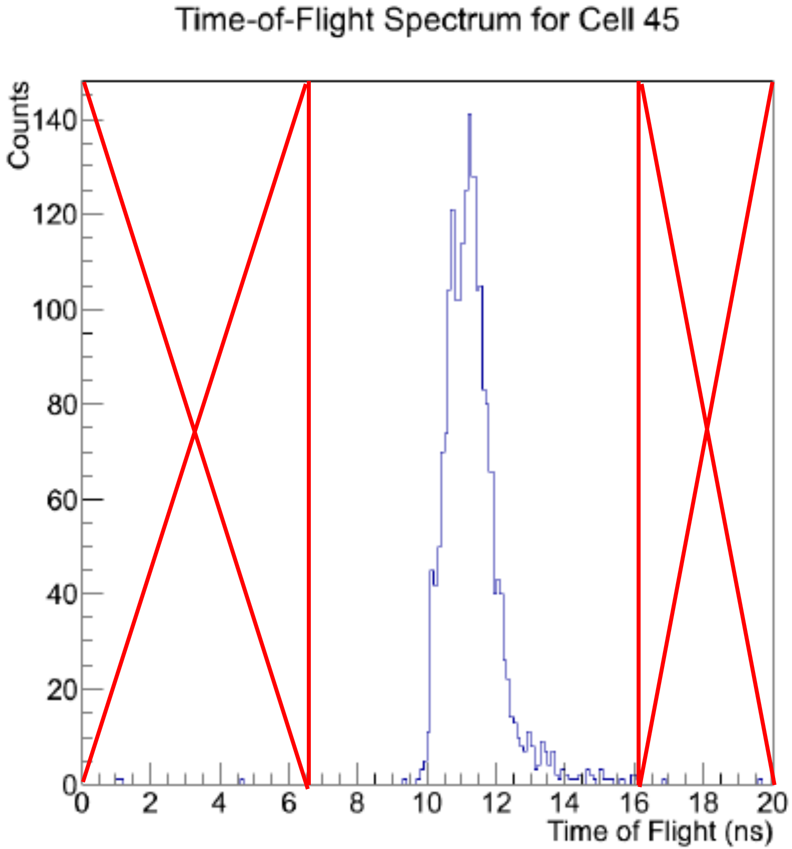

Analysis: Background Cut

Background:

photons (and other events) measured before the beam arrived.

Purpose:

eliminate any false-positives which may have passed the other cuts.

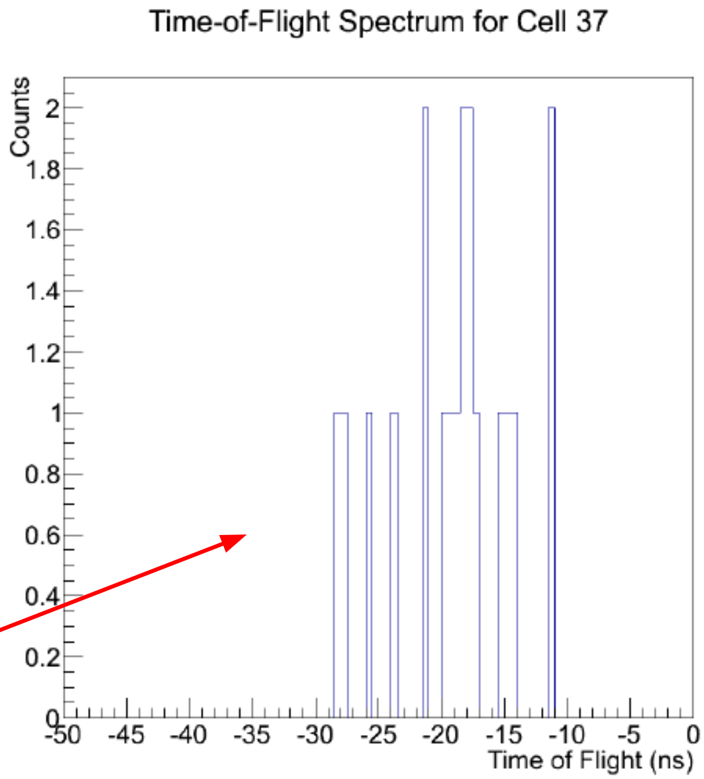

Rate is estimated from this plot, then scaled and subtracted from the yield

Analysis: Water Target Correction

Water Target Correction:

the neutron yield from the H_2O target was extracted and subtracted from the final D_2O yields.

Purpose:

eliminate any events which passed through the cuts but were not from deuteron photodisintegration.

Image credit: Kucuker (2010)

Analysis: Simulation Efficiency

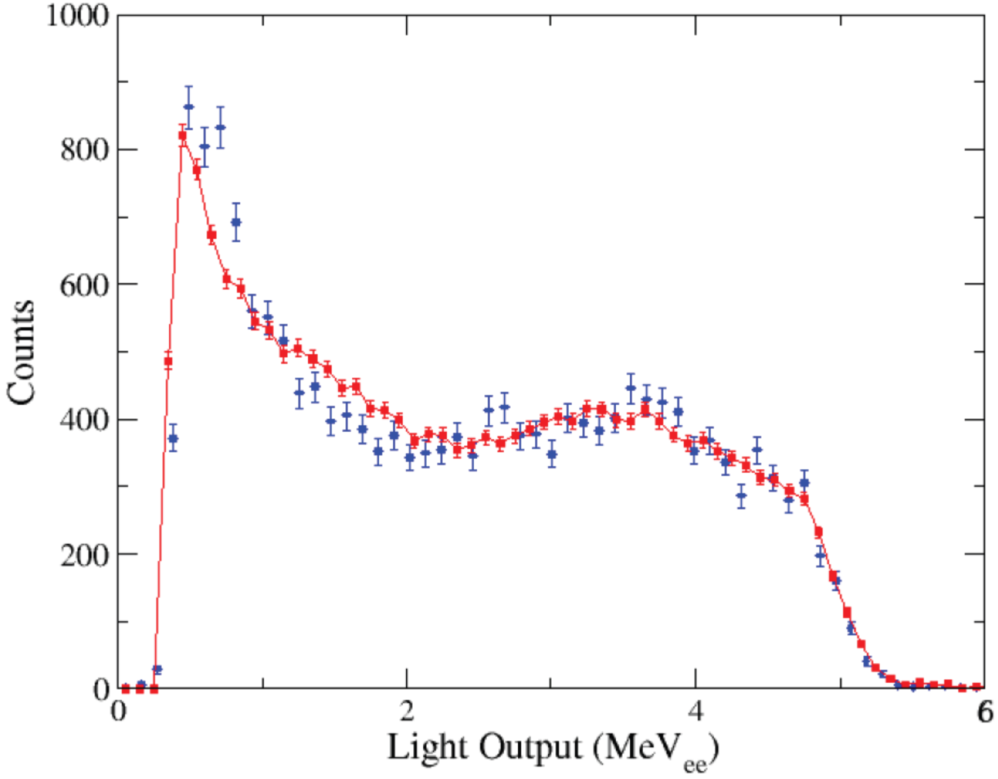

Analysis: Light Scaling Factors

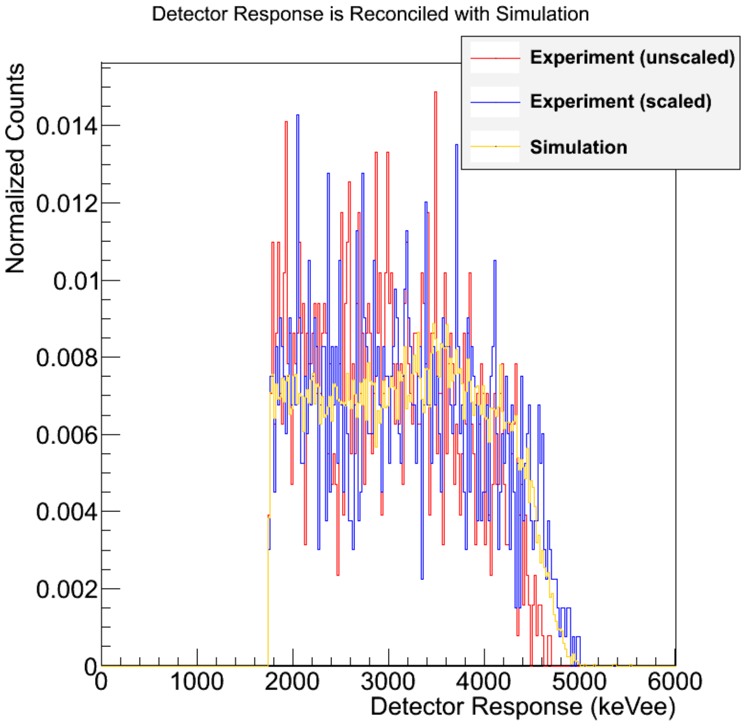

Analysis: Comparing to Theory

Cambi et al (1982) showed that the theoretical calculation can be parameterized in terms of associated Legendre polynomials:

$$\frac{d\sigma}{d\Omega}(\theta, \phi) = \sum_{k=0}^{n} A_k P_k^0(\cos\theta) + \sum_{k=2}^{n} B_k \Sigma_l P_k^2(\cos\theta)\cos 2\phi$$

Analysis: Comparing to Theory

Cambi et al (1982) showed that the theoretical calculation can be parameterized in terms of associated Legendre polynomials:

$$\frac{d\sigma}{d\Omega}(\theta,\phi) = \sum_{k=0}^{n} A_k P_k^0(\cos\theta) + \sum_{k=2}^{n} B_k \Sigma_l P_k^2(\cos\theta)\cos 2\phi$$

Angle || to beam direction

Analysis: Comparing to Theory

Cambi et al (1982) showed that the theoretical calculation can be parameterized in terms of associated Legendre polynomials:

$$\frac{d\sigma}{d\Omega}(\theta,\phi) = \sum_{k=0}^{n} A_k P_k^0(\cos\theta) + \sum_{k=2}^{n} B_k \Sigma_l P_k^2(\cos\theta)\cos 2\phi$$

Angle ⊥ to beam direction

Analysis: Comparing to Theory

Cambi et al (1982) showed that the theoretical calculation can be parameterized in terms of associated Legendre polynomials:

$$\frac{d\sigma}{d\Omega}(\theta, \phi) = \sum_{k=0}^{n} A_k P_k^0(\cos\theta) + \sum_{k=2}^{n} B_k \Sigma_l P_k^2(\cos\theta) \cos 2\phi$$

Analysis: Comparing to Theory

Cambi et al (1982) showed that the theoretical calculation can be parameterized in terms of associated Legendre polynomials:

$$\frac{d\sigma}{d\Omega}(\theta, \phi) = \sum_{k=0}^{n} A_k P_k^0(\cos\theta) + \sum_{k=2}^{n} B_k \Sigma_l P_k^2(\cos\theta) \cos 2\phi$$

Parameters: fit to, or calculated.

Analysis: Comparing to Theory

Cambi et al (1982) showed that the theoretical calculation can be parameterized in terms of associated Legendre polynomials:

$$\frac{d\sigma}{d\Omega}(\theta, \phi) = \sum_{k=0}^{n} A_k P_k^0(\cos\theta) + \sum_{k=2}^{n} B_k \Sigma_l P_k^2(\cos\theta) \cos 2\phi$$

Beam polarization ratio

Analysis: Comparing to Theory

The Legendre expansion parameters can be calculated from the reduced electric and magnetic multipoles given initial (*L*) and final (*L'*) multipolarities:

$$A_k \propto \delta_{N,even}(\mathcal{E}^L\mathcal{E}^{L'} + \mathcal{M}^L\mathcal{M}^{L'}) - \delta_{N,odd}(\mathcal{E}^L\mathcal{M}^{L'} + \mathcal{M}^L\mathcal{E}^{L'})$$

$$B_k \propto \delta_{N,even}(\mathcal{M}^L\mathcal{M}^{L'} - \mathcal{E}^L\mathcal{E}^{L'}) + \delta_{N,odd}(\mathcal{M}^L\mathcal{E}^{L'} - \mathcal{E}^L\mathcal{M}^{L'})$$

Analysis: Comparing to Theory

The Legendre expansion parameters can be calculated from the reduced electric and magnetic multipoles given initial (*L*) and final (*L'*) multipolarities:

$$A_k \propto \delta_{N,even}(\mathcal{E}^L\mathcal{E}^{L'} + \mathcal{M}^L\mathcal{M}^{L'}) - \delta_{N,odd}(\mathcal{E}^L\mathcal{M}^{L'} + \mathcal{M}^L\mathcal{E}^{L'})$$

$$B_k \propto \delta_{N,even}(\mathcal{M}^L\mathcal{M}^{L'} - \mathcal{E}^L\mathcal{E}^{L'}) + \delta_{N,odd}(\mathcal{M}^L\mathcal{E}^{L'} - \mathcal{E}^L\mathcal{M}^{L'})$$

Analysis: Comparing to Theory

We fit to the expansion by making a few adjustments:

$$\frac{d\sigma}{d\Omega}(\theta,\phi) = \sum_{k=0}^{n} A_k P_k^0(\cos\theta) + \sum_{k=2}^{n} B_k \Sigma_l P_k^2(\cos\theta)\cos 2\phi$$

$$\frac{d\sigma}{d\Omega} = \frac{\sigma}{4\pi}\left[1 + \sum_{k=1}^{4} a_k P_k^0(\cos\theta) + \sum_{k=2}^{4} e_k P_k^2(\cos\theta)\cos 2\phi \right.$$

$$\left. \ldots + \sum_{k=1}^{2} c_k P_k^1(\cos\theta)\cos\phi + \sum_{k=1}^{2} d_k P_k^1(\cos\theta)\sin\phi \right]$$

Target alignment terms

Analysis: Comparing to Theory

Then we map the Legendre expansion into a probability density function (PDF), f:

$$f = \frac{d\sigma}{d\Omega}\frac{1}{\sigma} = \frac{1}{4\pi}\Big[(1 - \sum_{k=1}^{4} a_k - 3e_2 - 6e_3 - 10e_4 - c_1 - \frac{3}{2}c_2 - d_1 - \frac{3}{2}d_2)\rho_{00}$$

$$\ldots + \sum_{k=1}^{4} a_k\rho_{0k} + 3e_2\rho_{22} + 6e_3\rho_{23} + 10e_4\rho_{24}$$

$$\ldots + c_1\rho_{11} + \frac{3}{2}c_2\rho_{12} + d_1\rho_{11'} + \frac{3}{2}d_2\rho_{12'}\Big]$$

Probabilities must be positive everywhere

Probabilities must integrate to unity

e.g. $\rho_{04} = (1 + P^0_4(\cos\theta))/(4\pi)$

Analysis: Comparing to Theory

Next, we use a Monte Carlo simulation of our experimental configuration to simulate the neutron yields, *N*, for each probability density function in:

$$
\begin{aligned}
N_d =& A[(1 - \sum_{k=1}^{4} a_k - 3e_2 - 6e_3 - 10e_4 - c_1 - \frac{3}{2}c_2 - d_1 - \frac{3}{2}d_2) N_{d,00}^{sim} \\
& \ldots + \sum_{k=1}^{4} a_k N_{d,0k}^{sim} + 3e_2 N_{d,22}^{sim} + 6e_3 N_{d,23}^{sim} + 10e_4 N_{d,24}^{sim} \\
& \ldots + c_1 N_{d,11}^{sim} + \frac{3}{2}c_2 N_{d,12}^{sim} + d_1 N_{d,11'}^{sim} + \frac{3}{2}d_2 N_{d,12'}^{sim}]
\end{aligned}
$$

Analysis: Comparing to Theory

Next, we use a Monte Carlo simulation of our experimental configuration to simulate the neutron yields, *N*, for each probability density function in:

$$\begin{aligned} N_d =& A[(1-\sum_{k=1}^{4} a_k - 3e_2 - 6e_3 - 10e_4 - c_1 - \frac{3}{2}c_2 - d_1 - \frac{3}{2}d_2)N_{d,00}^{sim} \\ &\ldots + \sum_{k=1}^{4} a_k N_{d,0k}^{sim} + 3e_2 N_{d,22}^{sim} + 6e_3 N_{d,23}^{sim} + 10e_4 N_{d,24}^{sim} \\ &\ldots + c_1 N_{d,11}^{sim} + \frac{3}{2}c_2 N_{d,12}^{sim} + d_1 N_{d,11'}^{sim} + \frac{3}{2}d_2 N_{d,12'}^{sim}] \end{aligned}$$

Simulated yields

Analysis: Comparing to Theory

Finally, we fit our experimental neutron yield for detector, *d*, to the function:

$$\begin{aligned}
N_d =& A[(1-\sum_{k=1}^{4} a_k - 3e_2 - 6e_3 - 10e_4 - c_1 - \frac{3}{2}c_2 - d_1 - \frac{3}{2}d_2)N_{d,00}^{sim} \\
&\ldots + \sum_{k=1}^{4} a_k N_{d,0k}^{sim} + 3e_2 N_{d,22}^{sim} + 6e_3 N_{d,23}^{sim} + 10e_4 N_{d,24}^{sim} \\
&\ldots + c_1 N_{d,11}^{sim} + \frac{3}{2}c_2 N_{d,12}^{sim} + d_1 N_{d,11'}^{sim} + \frac{3}{2}d_2 N_{d,12'}^{sim}]
\end{aligned}$$

Analysis: Comparing to Theory

Finally, we fit our experimental neutron yield for detector, *d*, to the function:

$$
\begin{aligned}
N_d = A[(1 - \sum_{k=1}^{4} a_k - 3e_2 - 6e_3 - 10e_4 - c_1 - \frac{3}{2}c_2 - d_1 - \frac{3}{2}d_2)N_{d,00}^{sim} \\
\ldots + \sum_{k=1}^{4} a_k N_{d,0k}^{sim} + 3e_2 N_{d,22}^{sim} + 6e_3 N_{d,23}^{sim} + 10e_4 N_{d,24}^{sim} \\
\ldots + c_1 N_{d,11}^{sim} + \frac{3}{2}c_2 N_{d,12}^{sim} + d_1 N_{d,11'}^{sim} + \frac{3}{2}d_2 N_{d,12'}^{sim}]
\end{aligned}
$$

We have 88 detectors and 12 fit parameters.

Analysis: Comparing to Theory

Example ($P_4^0(\cos\theta)$):

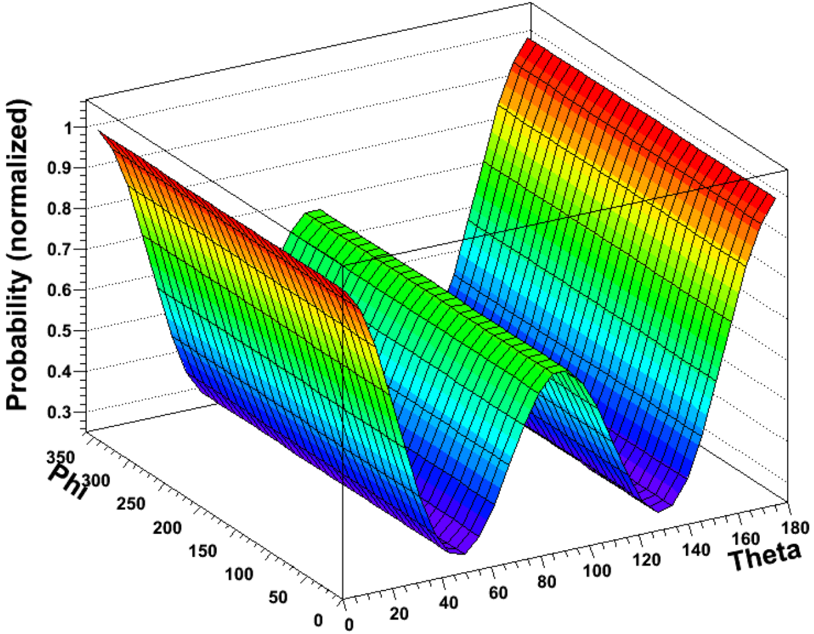

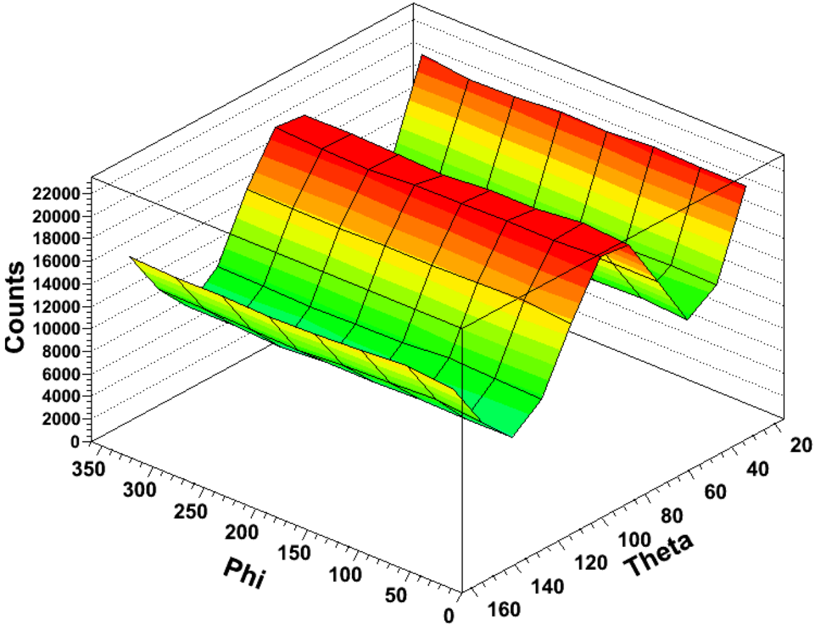

PDF: $\rho_{04} = (1 + P_4^0(\cos\theta))/(4\pi)$

Simulated Neutron Yield, $N_{d,01}^{sim}$

Analysis: Comparing to Theory

Summary

The theoretical and experimental data can be expressed as an expansion of associated Legendre polynomials.

We map the associated Legendre polynomials into probability density functions, then simulate them to see what neutron yields they *should* produce in our detectors.

$d\sigma/d\Omega(\theta,\varphi)$ and $\Sigma(\theta,\varphi)$

Finally, we fit our experimental results to the simulated yields to extract the parameters for the associated Legendre polynomial expansion and compare to theory.

Results: Total Cross Section

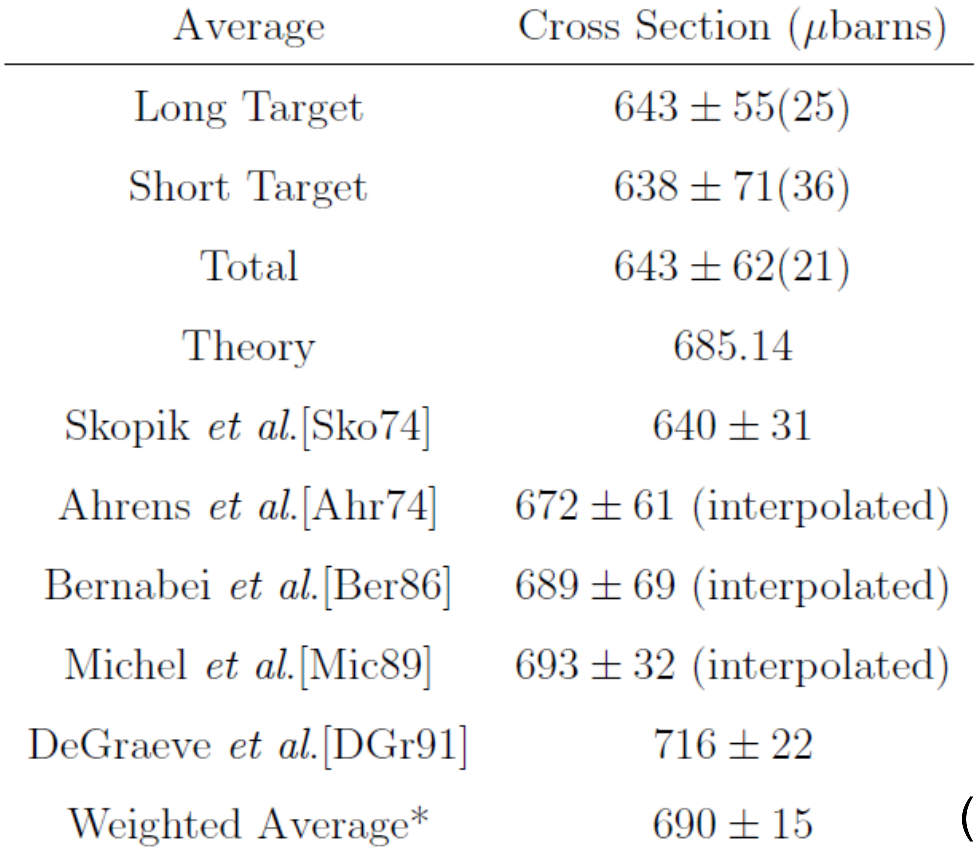

Average	Cross Section (μbarns)
Long Target	$643 \pm 55(25)$
Short Target	$638 \pm 71(36)$
Total	$643 \pm 62(21)$
Theory	685.14
Skopik *et al.*[Sko74]	640 ± 31
Ahrens *et al.*[Ahr74]	672 ± 61 (interpolated)
Bernabei *et al.*[Ber86]	689 ± 69 (interpolated)
Michel *et al.*[Mic89]	693 ± 32 (interpolated)
DeGraeve *et al.*[DGr91]	716 ± 22
Weighted Average*	690 ± 15

(random error only)

Results: Total Cross Section

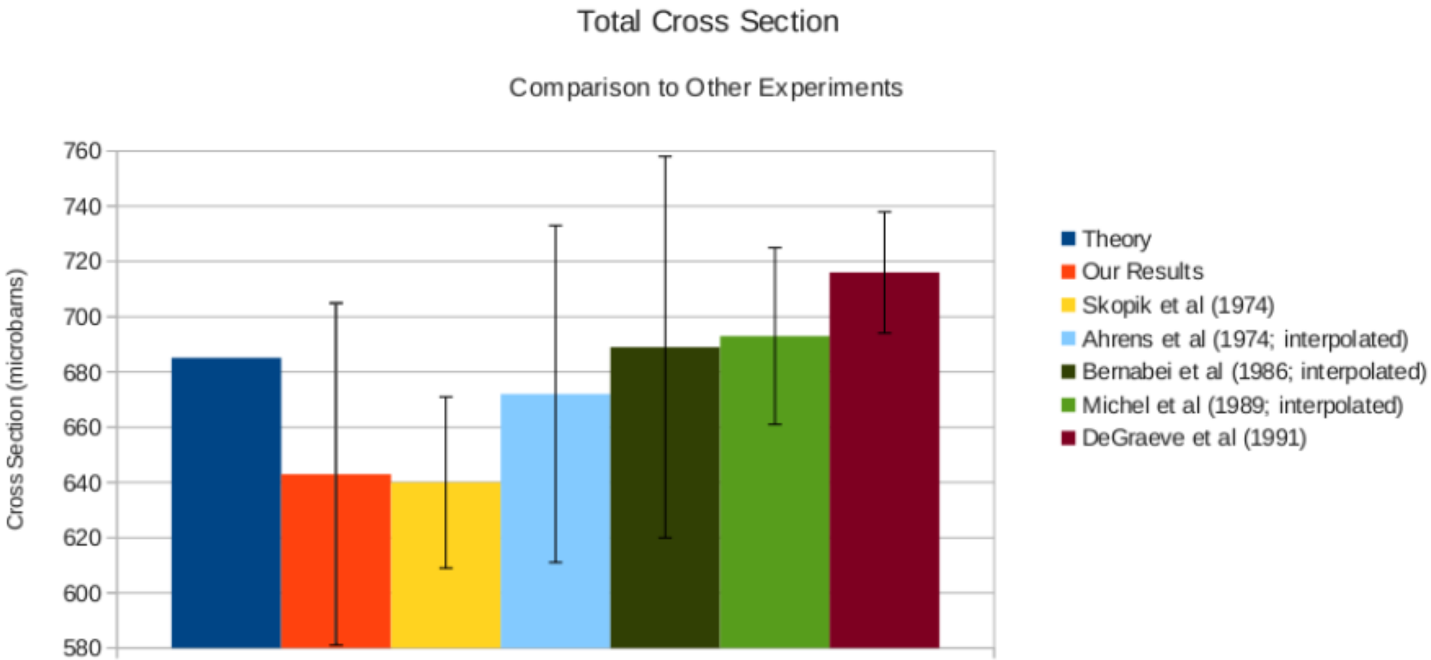

Results: Parameters

$$\frac{d\sigma}{d\Omega} = \frac{\sigma}{4\pi}\left[1 + \sum_{k=1}^{4} a_k P_k^0(\cos\theta) + \sum_{k=2}^{4} e_k P_k^2(\cos\theta)\cos 2\phi\right]$$

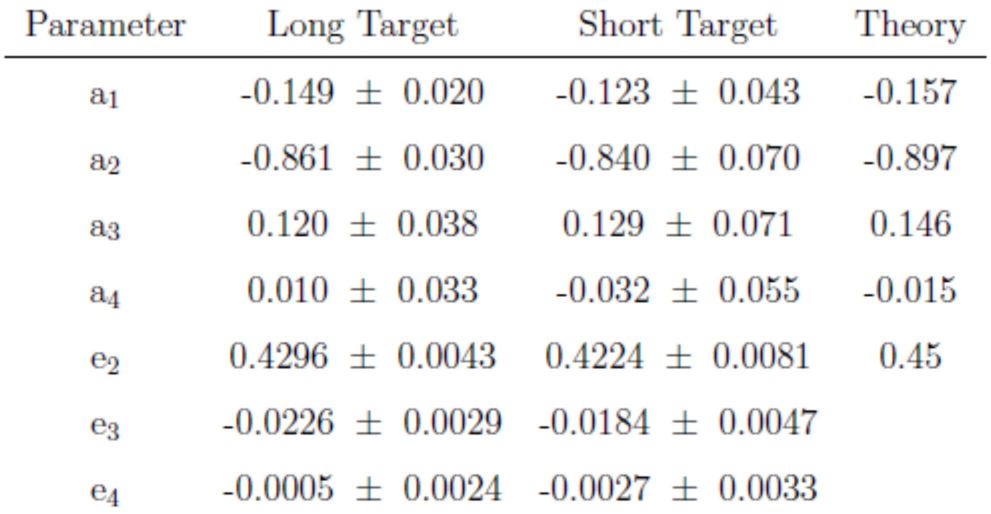

Parameter	Long Target	Short Target	Theory
a_1	-0.149 ± 0.020	-0.123 ± 0.043	-0.157
a_2	-0.861 ± 0.030	-0.840 ± 0.070	-0.897
a_3	0.120 ± 0.038	0.129 ± 0.071	0.146
a_4	0.010 ± 0.033	-0.032 ± 0.055	-0.015
e_2	0.4296 ± 0.0043	0.4224 ± 0.0081	0.45
e_3	-0.0226 ± 0.0029	-0.0184 ± 0.0047	
e_4	-0.0005 ± 0.0024	-0.0027 ± 0.0033	

Results: Parameterization

Correlation matrix

Lots of unexpectedly strong correlations e.g.

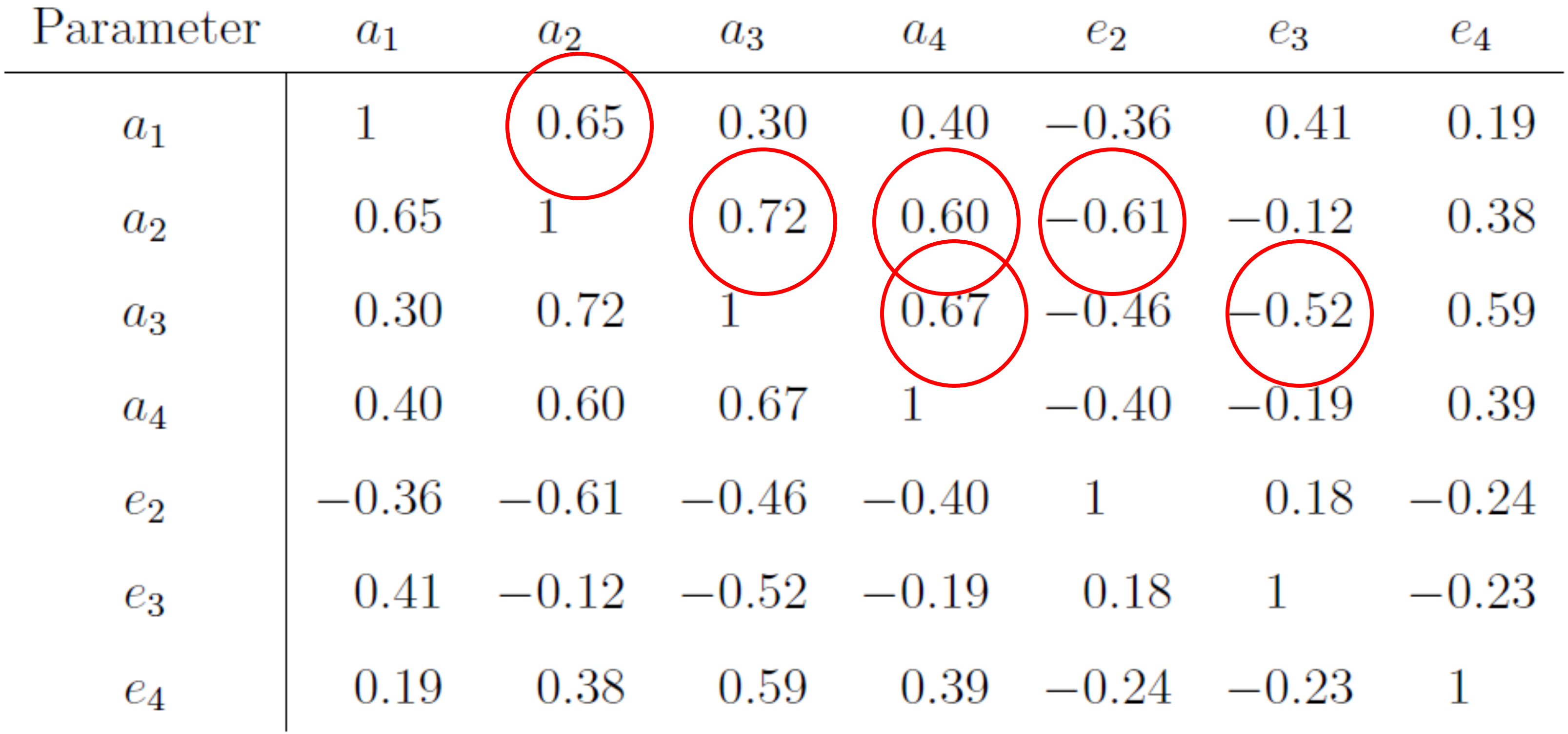

Parameter	a_1	a_2	a_3	a_4	e_2	e_3	e_4
a_1	1	0.65	0.30	0.40	−0.36	0.41	0.19
a_2	0.65	1	0.72	0.60	−0.61	−0.12	0.38
a_3	0.30	0.72	1	0.67	−0.46	−0.52	0.59
a_4	0.40	0.60	0.67	1	−0.40	−0.19	0.39
e_2	−0.36	−0.61	−0.46	−0.40	1	0.18	−0.24
e_3	0.41	−0.12	−0.52	−0.19	0.18	1	−0.23
e_4	0.19	0.38	0.59	0.39	−0.24	−0.23	1

Results: Parameterization

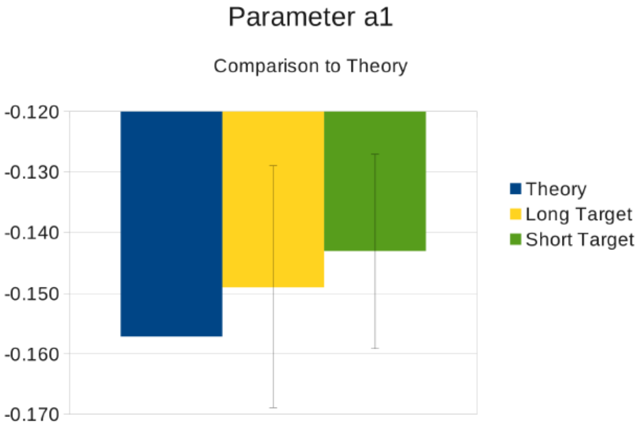
Parameter a1

Comparison to Theory

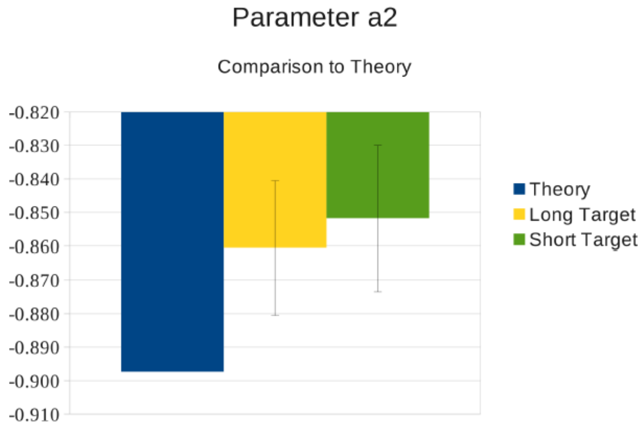
Parameter a2

Comparison to Theory

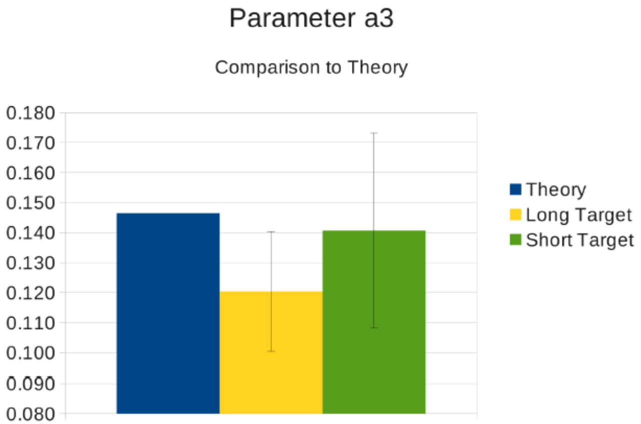
Parameter a3

Comparison to Theory

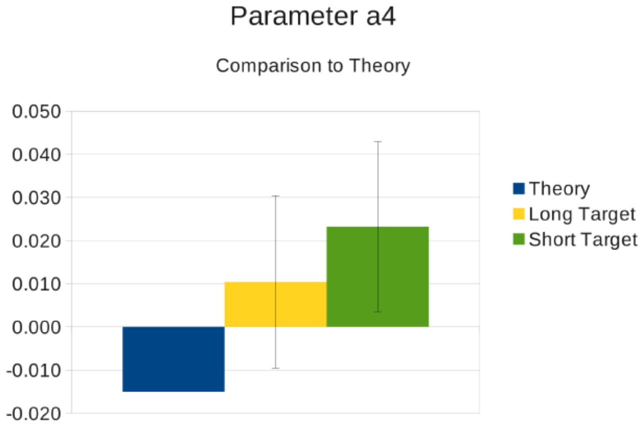
Parameter a4

Comparison to Theory

Results: Parameterization

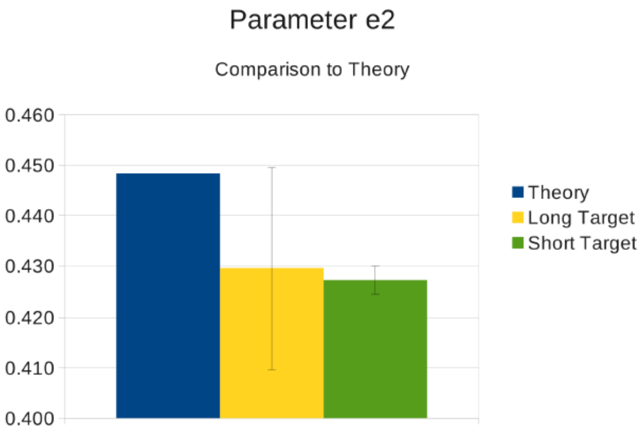
Parameter e2

Comparison to Theory

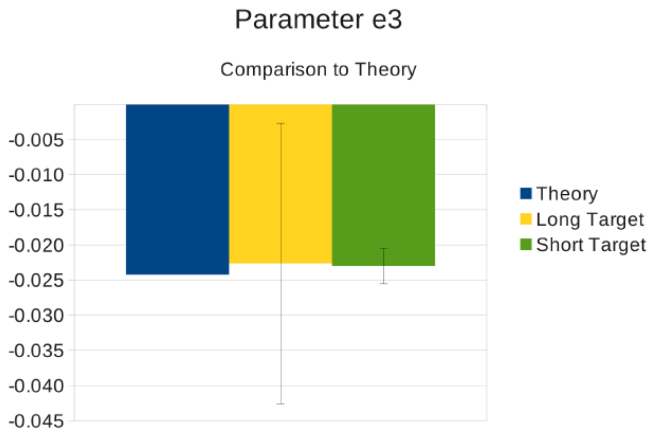
Parameter e3

Comparison to Theory

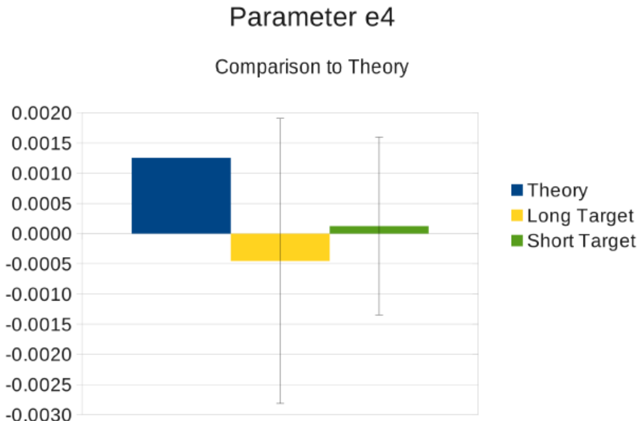
Parameter e4

Comparison to Theory

Results: θ-averaged Differential Cross Section

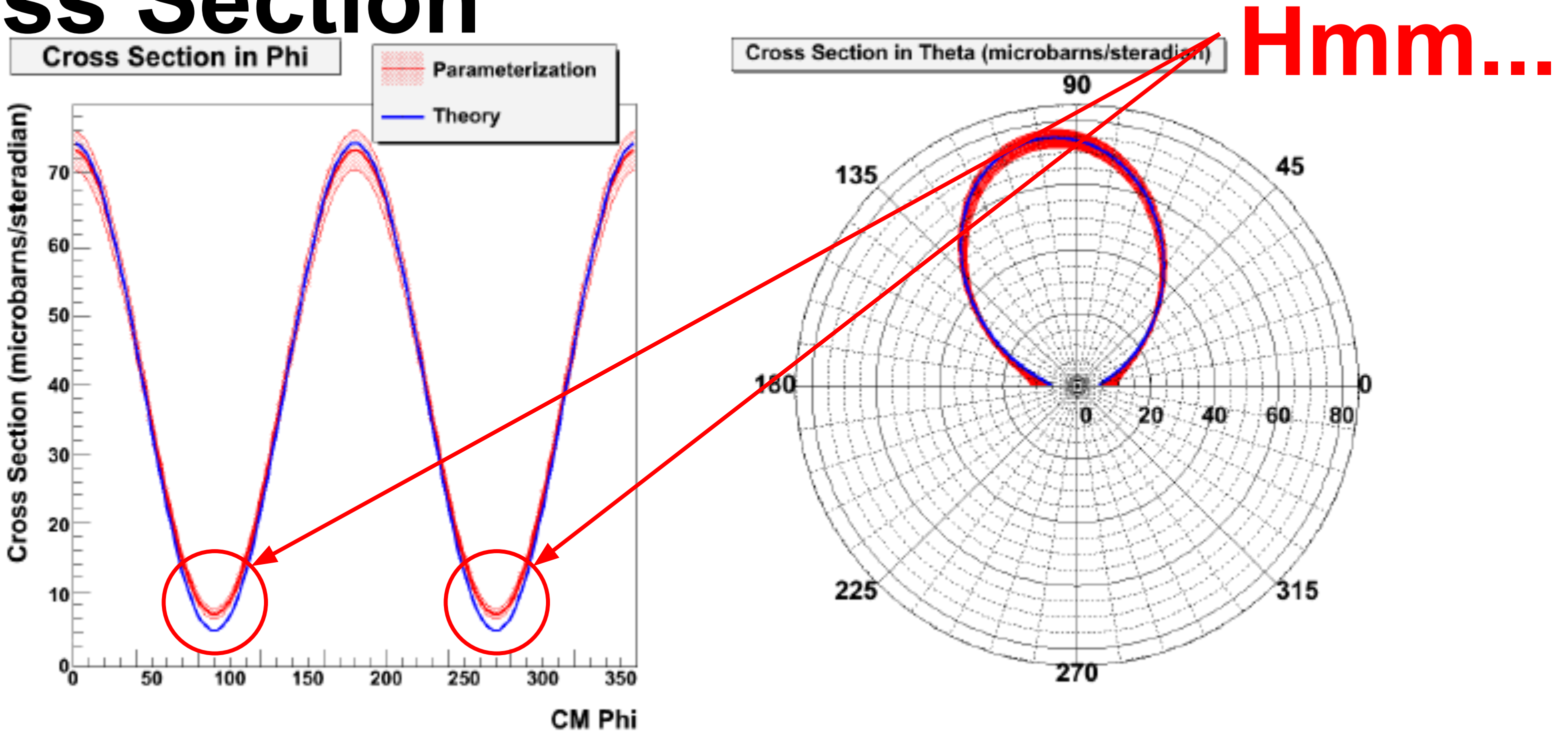

Note: this is an interpolation/extrapolation from the parameterization!

Results: Differential Cross Section

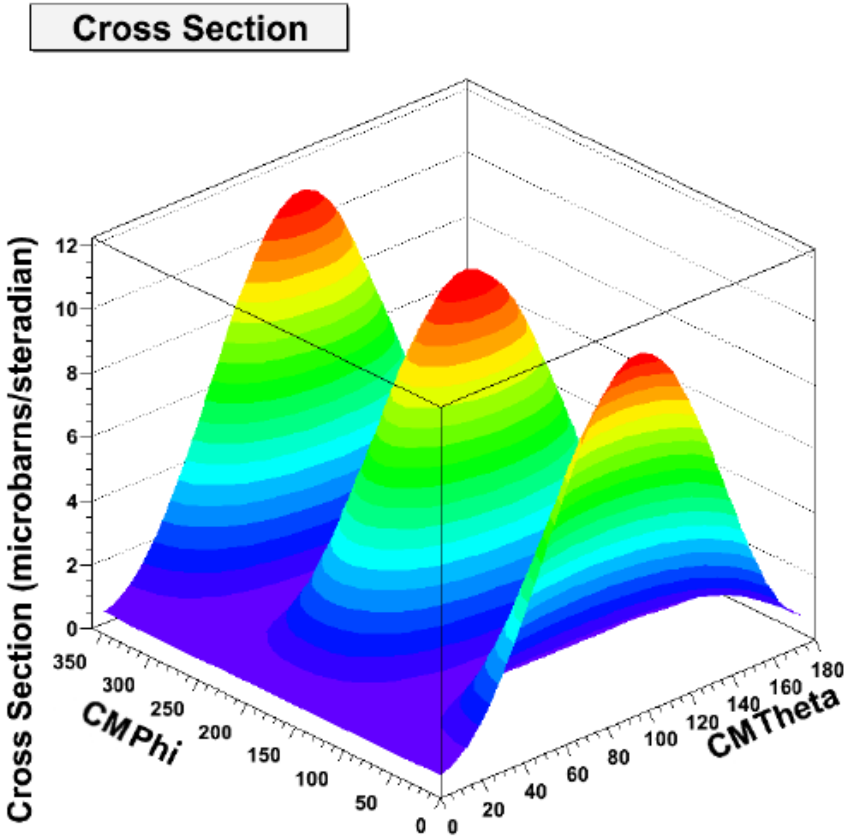

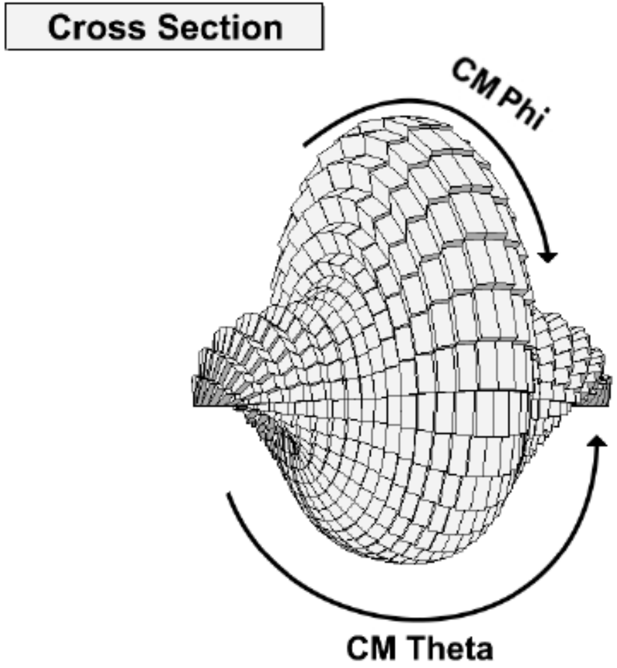

Sources of Error

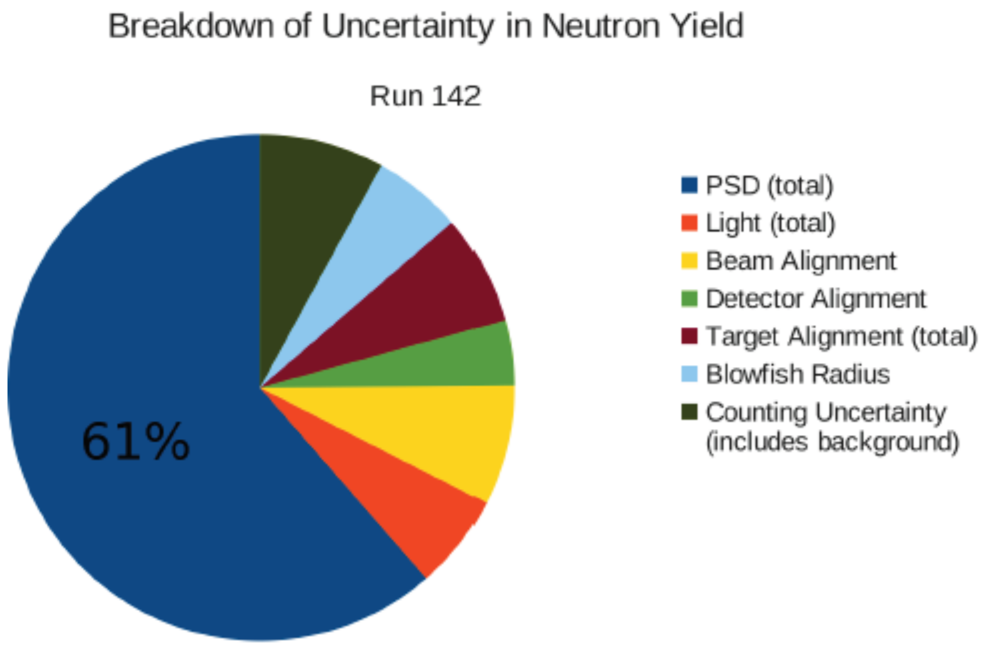

Sources of Error